Journal of Energy Storage 68 (2023) 107772

Contents lists available at ScienceDirect

Journal of Energy Storage

journal homepage: www.elsevier.com/locate/est

Review article

An overview of TiFe alloys for hydrogen storage: Structure, processes, properties, and applications

Huang Liu [a,b], Jingxi Zhang [a,c], Pei Sun [a], Chengshang Zhou [a,b,*], Yong Liu [b,**], Zhigang Zak Fang [a,**]

[a] Department of Materials Science and Engineering, The University of Utah, Salt Lake City, UT 84112-0114, United States
[b] State Key Laboratory of Powder Metallurgy, Central South University, Changsha, Hunan 410083, PR China
[c] School of Metallurgy and Environment, Central South University, Changsha, Hunan 410083, PR China

ARTICLE INFO

Keywords:
Hydrogen storage
Metal hydrides
TiFe alloy
Synthesis methods
Activation properties
Applications

ABSTRACT

Hydrogen-based energy systems offer potential solutions for replacing fossil fuels in the future. However, the practical utilization of hydrogen energy depends partly on safe and efficient hydrogen storage techniques. The development of hydrogen storage materials has attracted extensive interest for decades. Solid-state hydrogen storage systems based on metal hydride materials provide great promises for many applications. Recently, interest has been revived in TiFe alloys as a prime candidate for stationary hydrogen storage material. The advantages of TiFe alloys over some of the other solid metal hydrides include that it can hydrogenate and dehydrogenate at near room temperature under near atmospheric pressures and that it is a low-cost material because there are abundant supplies of Fe and Ti on the earth's crust. However, the TiFe alloy must be activated at relatively high temperatures (400–450 °C) and high pressure of hydrogen (65 bar) before it can be hydrogenated, which is a hindrance to the industrial-scale application of TiFe alloys. The materials science community on hydrogen storage materials has conducted and reported considerable amounts of studies on TiFe-based alloys. In this work, we provided a comprehensive review of TiFe-based alloys. The fundamentals and synthesis approaches of TiFe-based alloys were summarized. The activation properties of TiFe-based alloys including the understanding of the activation mechanisms and the methods for improving the activation kinetics were reviewed. Moreover, the cycle stability and anti-poisoning ability were discussed. Finally, the potential applications and the perspective of TiFe-based alloys were introduced.

1. Introduction

Hydrogen, as the most abundant element in nature, has the highest energy density by weight. Hydrogen is considered an ideal candidate for renewable energy carriers due to its ability to store and utilize energy in environmentally benign forms [1–4]. The concept of the hydrogen economy visioned the infrastructure that replaced fossil fuels with hydrogen to support the energy demands of society [5–7]. However, there are significant technological challenges that must be overcome before hydrogen-based energy systems can become a major contributor to the world's overall energy supply chain. One of the critical challenges is the methods for hydrogen storage. It is necessary to develop a reliable, low cost and efficient hydrogen storage system for moving towards an energy economy based on hydrogen.

To date, numerous hydrogen storage systems and techniques have been proposed for mobile and stationary hydrogen applications including the physical storage and material-based storage of hydrogen [7–9]. Physical storage methods of hydrogen include high-pressure compressed gas, cryogenic compressed gas, and liquid-state hydrogen storage [10]. Compressed gas or liquid hydrogen has the advantage of high gravimetric storage capacity. However, the physical storage methods usually involve considerable energy penalties due to the energy-consuming process of gaseous compression or liquefaction [11]. The compressed hydrogen storage consumes ~10% of energy. The energy consumption of liquid hydrogen storage can be up to 40% due to the liquefication at a relatively low temperature (−253 °C) [12,13]. Material-based hydrogen storage methods include physisorption adsorbents such as nano-porous carbon [14,15], metal-organic frameworks

* Correspondence to: C. Zhou, Department of Materials Science and Engineering, The University of Utah, Salt Lake City, UT 84112-0114, United States.
** Corresponding authors.
E-mail addresses: chengshang.zhou@csu.edu.cn (C. Zhou), yonliu@csu.edu.cn (Y. Liu), zak.fang@utah.edu (Z.Z. Fang).

https://doi.org/10.1016/j.est.2023.107772
Received 21 March 2023; Received in revised form 14 May 2023; Accepted 18 May 2023
Available online 1 June 2023

(MOFs) [16,17], and covalent-organic frameworks (COFs) [18,19]. The physisorption of hydrogen molecules relies on weak van der Waals forces, and thus low temperatures (−196 °C) and high pressures are generally required for significant adsorption [20]. Despite these physisorption adsorbents store hydrogen reversibly with rapid kinetics, low gravimetric capacity and the requirement of the cryogen conditions impede its practical application [11]. Metal oxides and mixed metal oxides with unique nanostructures also have been investigated as host physisorption materials for hydrogen storage, such as SnO_2 porous microspheres and $NiAl_2O_4$/NiO nanocomposites [21–24]. Although metal oxides and mixed metal oxides can be potentially utilized as a host material for hydrogen storage, these kinds of materials still suffer from the shortcomings in homogeneous nucleation, production cost, appropriate surface area and high catalytic activity [22]. Another form of material-based hydrogen storage is chemisorption, hydrogen molecules are split into atoms and hydrogen atoms react with solids to form hydrides [11,13]. The hydrides for hydrogen storage including metal/alloy hydrides such as MgH_2 [25,26], VH_2 [27,28], $TiFeH_2$ [29–31], and $LaNi_5H_6$ [32,33], complex metal hydrides such as $NaAlH_4$ [34], $LiAlH_4$ [35], $LiBH_4$ [36], and chemical hydrides such as ammonia (NH_3), ammonia borane (NH_3BH_3), methanol (CH_3OH), and DME (CH_3OCH_3) [37,38]. The complex hydrides suffer from the poor reversibility and complexity of hydrogen sorption reactions, and the potential applications of chemical hydrides were also hindered by high decomposition energy barrier or deactivation of catalysts [11,39].

Among current hydrogen storage systems, solid-state hydrogen storage systems based on metal/alloy hydrides have advantages with respect to their high volumetric hydrogen storage capacity and safety [40]. The volumetric capacity of compressed hydrogen and liquid hydrogen is 40 g/L (at 70 MPa) and 71 g/L, respectively [41,42]. For complex hydrides, the volumetric capacity is ~70–150 g H_2/L, and for interstitial hydrides, the volumetric density could be up to ~100–150 g H_2/L [41,42]. In metal/alloy hydrides, hydrogen molecules bond into metal under moderate pressures, usually between 3 and 30 bar [11]. The considerably lower operation pressure leads to a safer hydrogen storage system [43]. However, lightweight metal hydrides with relatively high gravimetric hydrogen storage capacity either have high desorption temperatures, slow kinetics, or poor reversibility, such as LiH, MgH_2, and AlH_3. For instance, the desorption temperatures of LiH and MgH_2 are ~720 °C and ~330 °C, respectively [44]. And hydrogen storage by AlH_3 is not reversible, the direct hydrogen requires over 10^3 MPa at room temperature [45]. Therefore, metal hydrides that can reversibly store hydrogen at ambient conditions are more practical for stationary hydrogen storage. Table 1 summarizes different types of alloys that can reversibly store hydrogen at ambient temperature. These room-temperature hydrogen storage alloys typically have low reversible hydrogen capacities of ~2 wt%, which limits their potential for use in vehicle onboard hydrogen storage applications. However, due to their high volumetric density of hydrogen (>100 kg·H_2/m^3), they are promising candidates for stationary storage applications. The room-temperature hydrogen storage alloys are usually intermetallic compounds with the general formula of A_nB_m, where A is a high temperature hydride forming element, B is a non-hydride forming element, n and m are positive integer [46]. These intermetallics usually consist or partly consist of transition metals, and thus hydrogen-metal bonding and electronic conductivity exhibits a metallic character [30,47]. The thermodynamics of intermetallic hydrides formed by intermetallic generally follow the well-known Miedema's rule, i.e., the more stable an intermetallic compound is, the less stable the corresponding hydride and vice versa [48,49]. The combination of A and B site elements with certain stoichiometric enable the intermediate thermodynamics of intermetallic hydrides, such as AB, AB_2, AB_3 and AB_5 alloys [46]. The most extensive studied AB-type alloy is TiFe, where Ti is strong hydride forming element, and Fe is non-hydride forming elements. A number of AB_2 and AB_5-type room-temperature hydrogen storage alloys, such as $TiMn_2$, $TiCr_2$, and $LaNi_5$ are already used in submarine hydrogen tanks [50], fuel cell forklifts [51,52], and electrodes of nickel-metal hydride (Ni-MH) rechargeable batteries [53].

For stationary hydrogen storage applications, some room-temperature hydrogen storage alloys show great promise as part of either a thermal storage cycle or an electrolyzer-fuel cell cycle [50,59]. Typical examples of commonly known intermetallic compounds for stationary hydrogen storage are shown in Fig. 1 [59]. Alloys such as $MmNi_5$, TiFe, $LaNi_5$, $TiMn_{1.5}$, and alloys of similar composition are of interest for stationary applications, owing to their favorable thermodynamic properties [59].

As one of the prime candidates for stationary hydrogen storage application, TiFe, which was first developed at Brookhaven National Laboratory by Reilly et al. in 1974 [54], has recently regained the interest of the materials science community and industry [30,31,60]. It has the advantages of a high volumetric density (105 kg_{H_2}/m^3) and low

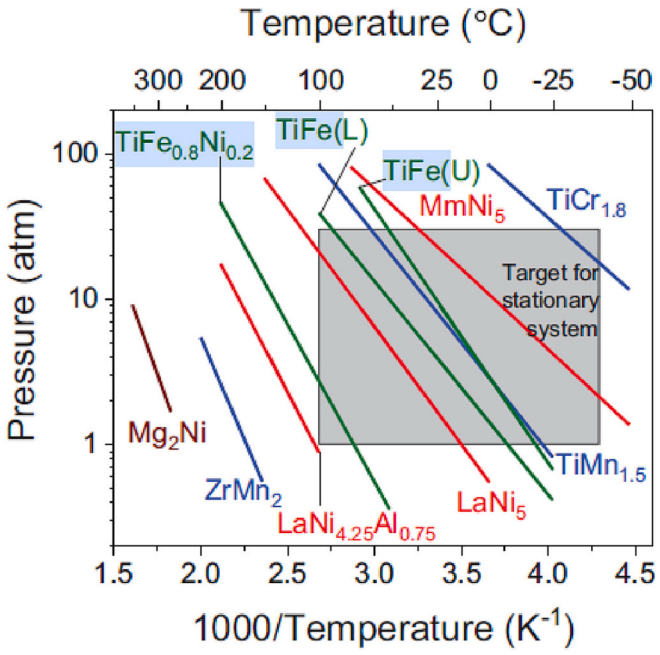

Fig. 1. Van't Hoff plots of decomposition plateau of common intermetallic hydrides with the estimated targets for stationary application (Reproduced with permission from ref. [59], Copyright © 2021 Modi and Aguey-Zinsou).

Table 1
The experimental hydrogen storage properties of room-temperature hydrogen storage alloys.

Type	Alloy composition	Maximum capacity (wt %)	Desorption enthalpy (kJ/mol·H_2^{-1})	Desorption plateau pressure (atm), temperature (°C)	Reference
AB_5	$LaNi_5$	1.5	28.3	8.5, 70	[45]
AB	TiFe	1.9	28.1	5.2, 30	[54]
AB_2	$TiMn_{1.5}$	1.9	28.7	8.4, 25	[55]
AB_3	$CaNi_3$	1.8	35.02	0.4, 20	[56]
BCC solid solution	$V_{0.48}Fe_{0.12}Ti_{0.15}Cr_{0.25}$	2.0	30.1	7.93, 22	[57]
High entropy alloy	TiZrCrMnFeNi	1.7	–	~1, 30	[58]

cost [30]. However, the requirement for activation at high temperatures (400–450 °C) and high pressure of hydrogen (65 bar) is a significant hindrance to its industrial-scale applications. Therefore, the vast majority of research has focused on understanding the activation mechanisms and finding ways to make it easier for activation.

The previous reviews by Sujan et al. [29], Dematteis et al. [30] and Zhang et al. [31] reviewed microstructure, hydrogenation properties, substitutional effects and modified treatments of TiFe-based alloys. In this review, we aim to provide a comprehensive understanding of hydrogen storage behavior and the recent developments of TiFe-based alloys. Firstly, the fundamentals of TiFe-based alloys were introduced. Secondly, the processes for the synthesis of TiFe alloys were reviewed. Then, we focused on the activation properties of TiFe-based alloys including the understanding of the mechanisms of the activation and the methods for improving the activation kinetics. Next, we summarized the cycle stability, anti-poisoning ability, and the potential applications of TiFe for stationary energy storage and even for transportation vehicles. Finally, the perspective of the TiFe in hydrogen storage areas was discussed.

2. Fundamentals of TiFe alloys

2.1. TiFe and its hydrides

The binary Fe—Ti phase diagram is shown in Fig. 2(a). It shows there are two stable intermetallic compounds, TiFe and $TiFe_2$. On the Ti-rich side, two phases are present: α-Ti and β-Ti with a maximum solubility of 21 at.% Fe. The single-phase region of TiFe is narrow, and the broadest is at the eutectic temperature of 1085 °C, with Ti content ranging from 49.7 to 52.5 at.%. Based on the Fe—Ti phase diagram (Fig. 2(a)), TiFe can be obtained during the cooling of the melt through the liquid + $TiFe_2$ → TiFe peritectic reaction at 1317 °C. TiFe can reversibly ab/desorb hydrogen at room temperature after activation treatment. However, $TiFe_2$ does not react with hydrogen [54].

TiFe crystallizes in a cubic CsCl-type (B2, space group *Pm-3m*) structure. Within the narrow single-phase composition range, the lattice parameters of TiFe extend from 2.972 to 2.978 Å depending on the Ti content (49.7–52.5 at.%) [61–64]. Generally, TiFe is a body-centered-cubic (bcc) cell with one formula unit per unit cell. Ti atoms reside in the center of the cube cell and Fe atoms are shared in the corner of the cell. Each cell contains 12 tetrahedral and 6 octahedral interstices [65]. However, contrary to bcc, the TiFe crystal system also has different kinds of configurations with two distinct cubic sublattices, the atoms are located at 1a sites (0,0,0), and 1b sites (0.5,0.5,0.5) [66]. H-atoms preferably occupy the interstitial octahedral sites rather than the tetrahedral sites. The octahedral interstices of the TiFe compound have two different configurations distinguished by surrounding atoms, i.e., [Ti4Fe2] and [Ti2Fe4] [65,67]. H-atoms prefer the [Ti4Fe2] site, which is associated with a smaller volume expansion [68].

The hydrogenation of TiFe results in the formation of one TiFe-H solid solution and two ternary hydrides: $TiFeH_{0.1}$, (α-phase, solid solution), $TiFeH_{1.04}$ (β-phase, hydride), and $TiFeH_{1.95}$ (γ-phase, hydride). The reactions which take place stepwise can be expressed as follows [69]:

$$TiFeH_{0.1} + H_2 \rightleftharpoons TiFeH_{1.04} \quad (1)$$

$$TiFeH_{1.04} + H_2 \rightleftharpoons TiFeH_{1.95} \quad (2)$$

$TiFeH_{1.04}$ has an orthorhombic structure with a P_{2221} space group, and $TiFeH_{1.95}$ has an orthorhombic structure with a *Cmmm* space group, as displayed in Fig. 2(b). The $TiFeH_{1.04}$ hydride corresponds to a structure where hydrogen atoms occupy the more stable octahedral sites [Ti4Fe2] of the TiFe compound. The $TiFeH_{1.95}$ hydride corresponds to a structure where hydrogen atoms occupy both kinds of octahedral sites, [Ti4Fe2] and [Ti2Fe4] [65,67,70]. $TiFeH_{1.04}$ and $TiFeH_{1.95}$ are gray metal-like solids with essentially the same appearance as the initial TiFe alloy [68]. These hydride phases are very brittle and easily degrade when exposed to air.

2.2. Thermodynamics

As demonstrated in Fig. 3, two distinct hydrides ($TiFeH_{1.04}$ and $TiFeH_{1.95}$) result in two separate plateaus. The Pressure-Composition-Temperature (PCT) isotherm of the TiFe-H system was first obtained by Reilly et al. [54], as shown in Fig. 3. The first plateau of the PCT curve was attributed to the formation of β-phase $TiFeH_{1.04}$. The second

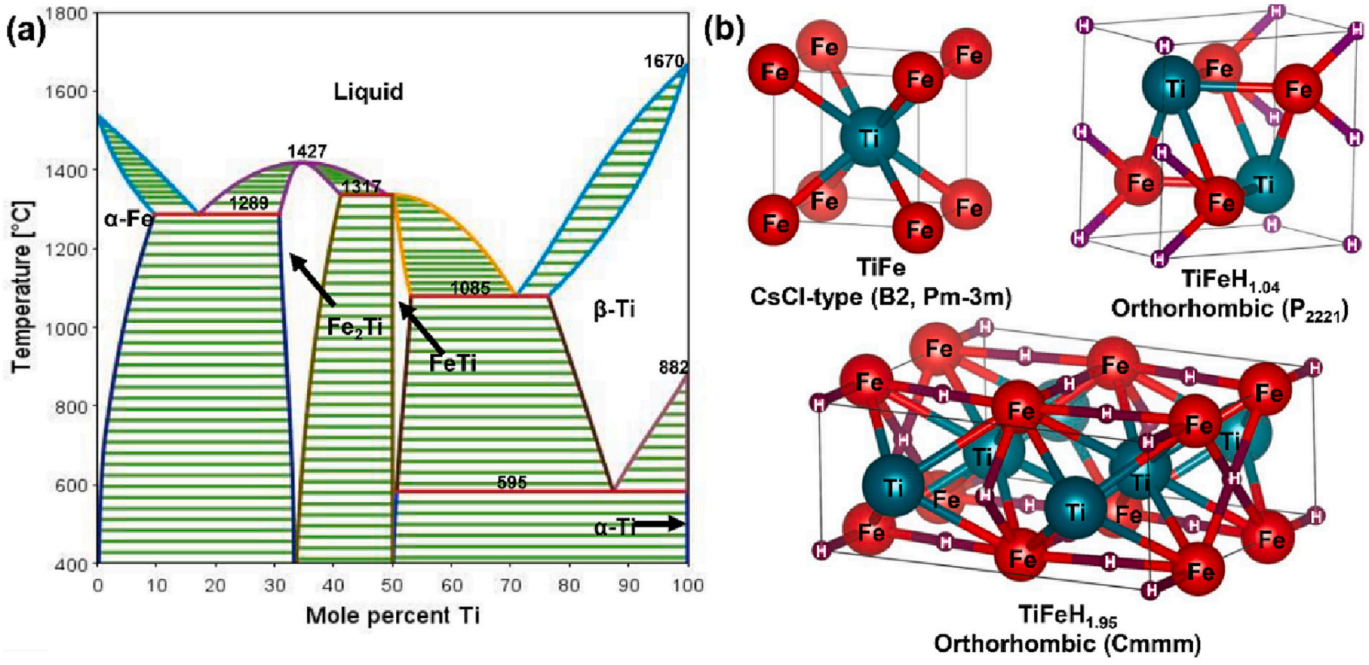

Fig. 2. (a) Phase diagram of binary Ti—Fe system, the phase stability domains according to Ti atomic percentage. (Reprinted with permission from ref. [71]. Copyright 2022 Elsevier). (b) Crystal structures of TiFe, TiFe-$H_{1.04}$, and TiFe-$H_{1.95}$.

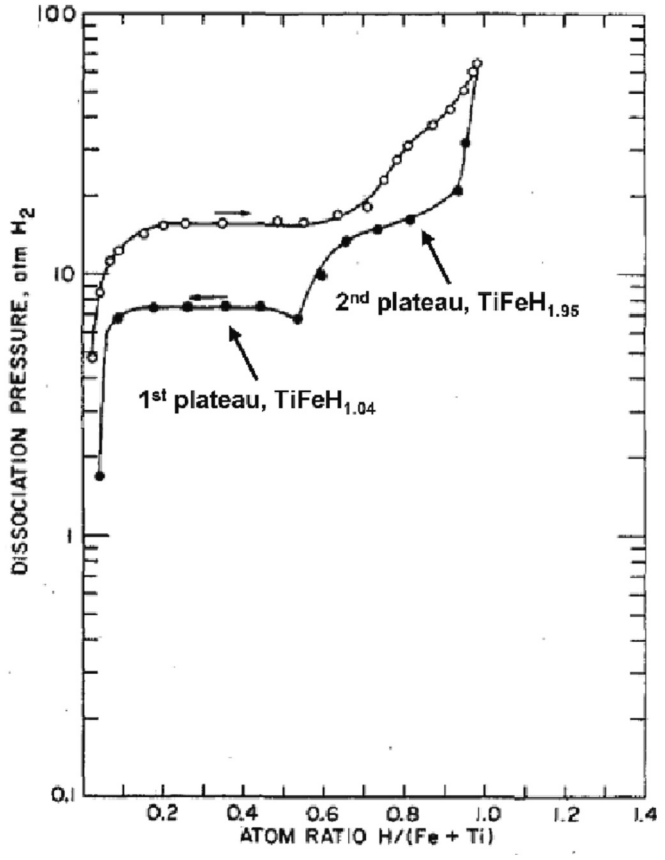

Fig. 3. The PCT isotherm for the TiFe-H system at 40 °C. (Reproduced with permission from ref. [54]. Copyright 1974 American Chemical Society).

plateau, which has a significant slope, was ascribed to the formation of γ-phase $TiFeH_{1.95}$. The occurrence of a double plateau implies a larger pressure range for the usage of TiFe in practical applications, and since the second plateau is found at relatively high pressure, it complicates the engineering of the hydrogen storage system.

Using the PCT results at different temperatures, and plotting the logarithm of the equilibrium pressures obtained against inverse temperature, the thermodynamics parameters can be derived by the van't Hoff equation:

$$ln(P_{eq}) = \frac{\Delta H}{RT} - \frac{\Delta S}{R} \quad (3)$$

where P_{eq} is the equilibrium pressure; R is the gas constant, $R = 8.314$ J/(mol·K); T is the experimental temperature; ΔH is the hydrogen sorption enthalpy; and ΔS is the hydrogen sorption entropy. ΔH is a measure of the bonding strength between hydrogen and metal atoms, it can vary over wide limits [65]. ΔS is rather constant, associated with the change from gaseous to solid hydrogen [65]. Reilly et al. [54] reported that the desorption enthalpy and entropy determined by the first plateaus are 28.1 kJ/(mol·H_2) and 106 J/(mol·K) respectively. Table 2 summarizes the hydrogen storage properties and thermodynamic parameters of TiFe.

The PCT of TiFe alloy (Fig. 3) also exhibits a significant hysteresis between hydrogen absorption and desorption cycles. The hydrogen ab/desorption equilibrium pressure difference also has a negative effect on the applications of TiFe alloys. This undesirable hysteresis can be slightly mitigated with the increase of hydrogen sorption cycles [72], but it cannot be eliminated. Goodell et al. [72] believed that this phenomenon may due to initial particle decrepitation prior to the formation of a relatively stable particle size, lattice strain and/or kinetic effects. It is worth noting that the addition of alloying elements (such as Mn, V, Cr, Co, Ni, etc.) could reduce the hysteresis effects [73–75]. Dermatitis et al.

Table 2
Experimental hydrogen storage properties and thermodynamic parameters of TiFe.

	Values [30,54,76]
Hydrogen storage capacity	
Gravimetric capacity, wt%	1.9
Volumetric capacity, kg_{H_2}/m^3	105
Energy density	
Gravimetric energy density, MJ/kg	2.3
Gravimetric energy density, MJ/dm^3	12.6
Thermodynamic parameters	
1st desorption plateau pressure at 30 °C, bar	5.2
Hydride desorption enthalpy, kJ/(mol·H_2)	28.1
Hydride desorption entropy, J/(mol·K)	106

[73] found that the hysteresis effects of Mn doped TiFe alloy may related with the difference in cell parameter. The hysteresis of TiFe-Mn alloy decreases with the enlargement of the TiFe cell parameters [73].

The thermodynamics of TiFe alloys could vary depending on the composition including oxygen content and microstructures due to different methods of synthesis and treatment. The thermodynamics of TiFe can also be tailored by alloying with the third element or multi-elements to optimize the operational pressure for matching versatile practical applications. However, most of the alloying will result in an increase in hydrogen sorption enthalpy values of TiFe, which implies more stable hydrides [30]. More recently, Fadonougbo et al. [81] investigated the effect of elemental substitution on the lattice contraction/expansion of $TiFe_{1-x}M_x$ alloys and subsequent monohydride decomposition energy using first-principles density functional (DFT) theory calculation with Al, Be, Co, Cr, Cu, Mn, and Ni as substitutional elements for Fe sites. A linear relationship between monohydride formation energy/enthalpy and plateau pressure was proposed (Fig. 4) [81].The thermodynamic variation by alloying of TiFe is reported to be associated with the lattice parameters. Based on Lundin's geometric model, larger radii of tetrahedral holes correlate to higher stability of their hydrides [77]. There is evidence of a linear relationship between the logarithm of the plateau pressure and the volume of the unit cell or interstitial sites of the TiFe-based alloy [78–80].

2.3. Activation behavior and mechanisms

When hydrogen is initially applied to TiFe, the hydrogenation reaction usually does not occur immediately, which can be attributed to the oxide film barrier present on the air-exposed surfaces. To overcome this issue, a process called activation is utilized, which involves applying significantly higher than equilibrium H_2 pressure to force the metal to hydride for the first time. Activation is an important consideration for many metal hydrides used in hydrogen storage [65]. Some of high entropy hydrogen storage alloys can be easily activated at room temperature without thermal treatment, such as $Ti_xZr_{2-x}CrMnFeNi$ (x = 0.4–1.6) and TiZrNbFeNi alloys [83,84]. For rare-earth-containing AB_5 and Mn-containing AB_2 intermetallic compounds, the incubation time could vary from seconds to days before the first hydrogen absorption begins at room temperature [65]. However, the activation of TiFe requires high temperatures and high pressure of hydrogen. An activation treatment at 400–450 °C and 65 bar of hydrogen was necessary for triggering the full hydrogen ab/desorption of TiFe alloys at room temperature [54]. Besides the harsh requirements for activation, TiFe alloys are easily deactivated by water vapor and oxygen contamination during material handling and processing [85–89]. Therefore, understanding the activation behavior and mechanisms of TiFe-based systems is crucial for their practical application.

TiFe is prone to oxidation due to its high affinity to oxygen. Extensive studies reported that the surface oxide layer hinders hydrogen

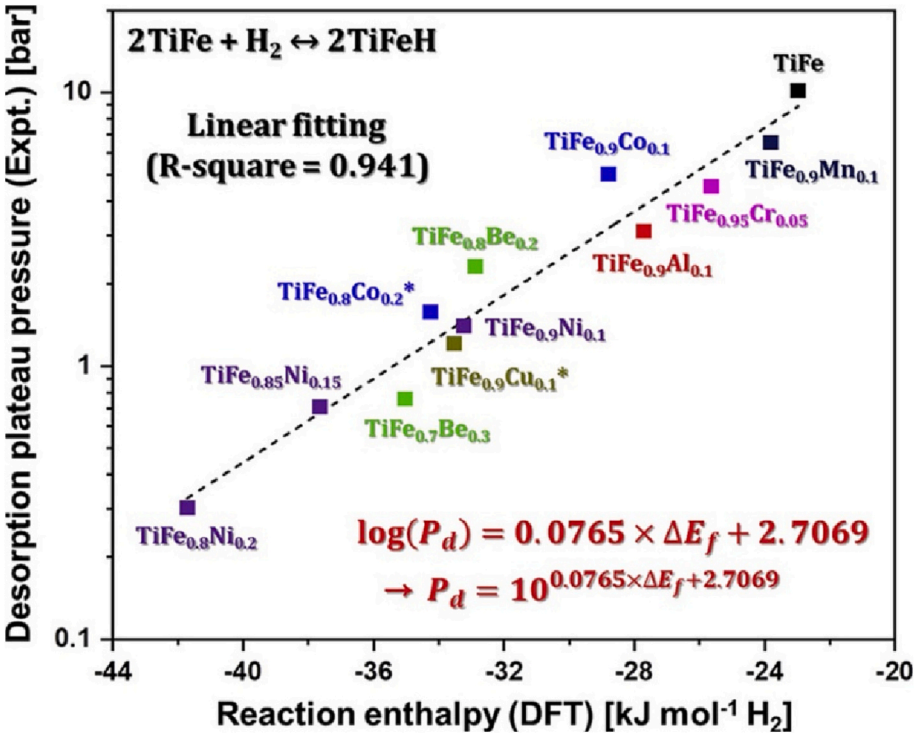

Fig. 4. The correlation between the experimentally measured desorption plateau pressure (at 50 °C) and dehydrogenation enthalpy of single-element alloyed TiFe (Reprinted with permission from ref. [81]. Copyright 2022 Elsevier).

penetration and interaction with TiFe, and thus high activation temperature becomes necessary [54,90–93]. Sandrock et al. [94] found that the thin oxygen-rich film of the air-exposed TiFe alloy is roughly 20–30 nm. The composition of the surface passivating layer is considered to be $Ti_7Fe_5O_2$, as identified by Matsumoto et al. [95]. However, Pande et al. [96] suggested that the composition of the oxygen-rich layer on the surface is Ti_3Fe_3O. And they believed the Ti_3Fe_3O impedes the hydrogen reaction with TiFe at the surface, due to Ti_3Fe_3O is not able to absorb hydrogen. In contrast, Schober et al. [91,107] reported that the surface of TiFe is composed of rutile TiO_2, ordered suboxide $FeTiO_x$ and $TiFe_2$. Recently, Park et al. [97] reported that an amorphous thin oxide film (~6 nm) covered the surface of as-cast TiFe, as demonstrated by TEM results in Fig. 5(a), (b), and (c). The XPS surface depth profile of as-cast TiFe (Fig. 5(d)) confirmed the existence of the oxide layer which is composed of complex Ti–Fe-oxide. The discrepancies in the reported surface compositions were attributed to the oxygen impurities content of raw materials, synthesis atmosphere, and heat treatment atmosphere [98].

Although numerous efforts have been made to comprehend the fundamental principles that underlies the activation behavior. The proposed activation processes include chemical reduction by hydrogen, surface segregation induced by high temperature, surface oxides dissolution into the bulk, catalytic effects by surface Fe clusters, hydrogen pathway through ternary TiFe oxides of the surface, and lower fracture toughness by secondary phases. Among these, surface segregation of TiFe is the most extensively reported explanation of activation behavior. Surface segregation was first proposed to explain the superior activation properties of $LaNi_5$ [99]. La diffuses to the surface and oxidizes, while metallic Ni precipitates remain and catalyze the dissociation of molecular hydrogen, thus enabling the $LaNi_5$ to be easily activated at room temperature [99,100]. However, the surface segregation of TiFe only occurred at high temperatures [90,101,102]. During the activation at high temperatures under the hydrogen atmosphere, the surface segregation and chemical reduction result in the conversion of initially passivating surface oxide into a mixture of TiO_2 and Fe [92,103]. The clean sub-surfaces and Fe precipitates served as active sites for the activation of TiFe alloys [92,103]. And the presence of oxygen promotes surface segregation [104], and surface segregation may help the oxide

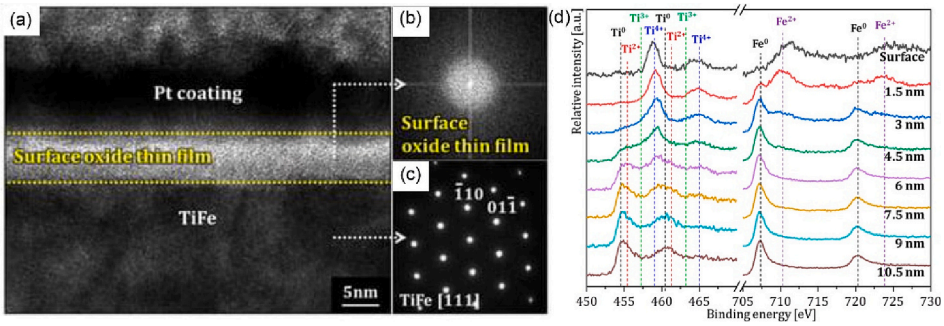

Fig. 5. Structural and surface characterization of the as-cast TiFe alloy: (a) cross-sectional transmission electron microscopy (TEM), (b) selected area diffraction patterns (SADPs) of thin surface oxide film, (c) SADPs of the TiFe bulk, and (d) X-ray photoelectron spectroscopy (XPS) depth profile (Reproduced with permission from [97], published by MDPI, 2022).

layer transform to the Ti_4Fe_2O-phase, which is known to absorb hydrogen, thereby overcoming the barrier at the surface [96,98].

Surface Fe precipitate was believed to be the crucial component for activation, but its catalytic effect is controversial. Surface Fe clusters in the metallic state generated by surface segregation and chemical reduction are believed to be active sites, which promote the dissociation of the hydrogen molecule. Blasius et al. [102] confirmed that the hydrogen activation process causes the formation of Fe clusters in the vicinity of the surface by Mossbauer studies. Recently, Edalati et al. [105] detected Fe-rich clusters on the TiFe surfaces and claimed that Fe-rich clusters can act as catalysts and thus facilitate activation. In contrast, Fruchart et al. [106] believed that the catalytic role of surface Fe precipitates is questioned, due to Fe dissolving hydrogen poorly and its catalytic properties are not remarkable.

Besides surface segregation and chemical reduction, surface oxide dissolution has proposed as one of the explanations for the activation of TiFe alloys. Schober et al. [107] believed that the surface oxide of TiFe dissolves into the subsurface layer at high temperatures. Yang et al. [108] observed the surface Ti oxide dissolved into the TiFe matrix by XPS. The oxygen dissolution is believed to occurred only at high temperatures under hydrogen pressure [108].

The secondary oxide phase of TiFe alloy is also correlates with the activation behavior. Ternary Ti-Fe-O oxides are always present in the TiFe-based alloys, due to the oxygen impurities of raw materials and oxygen uptake during the synthesis process. A typical example of secondary oxygen-containing phases of TiFe alloys is $Ti_4Fe_2O_x$ [109,110]. $Ti_4Fe_2O_x$ can absorb hydrogen at room temperature without thermal treatment [111]. Rupp et al. [111] reported that bulk $Ti_4Fe_2O_{0.4}$ reacted easily with hydrogen at 298 K under hydrogen at 4 MPa. It is believed that $Ti_4Fe_2O_x$ formed in the TiFe alloy acts as an activation promotor [106,112]. Venkert et al. [112] assumed that hydrogen penetrates through the surface $Ti_4Fe_2O_x$ into the bulk TiFe and enabled the activation.

The activation of TiFe alloy is also attributed to the lower fracture toughness of the alloy particle influenced by secondary phases. Sandrock et al. [94] found that oxygen promotes the formation of $Fe_{3-x}Ti_{3-x}O_y$, $TiFe_2$, and α-Ti or β-Ti secondary phases in the TiFe alloy. These secondary phases could facilitate the pulverization and provide preferential nucleation sites during hydriding and thus help activation [94]. Schlapbach et al. [92] believed the secondary phase lowers the fracture toughness and favors the disintegration that shortens the hydrogen diffusion path.

Despite a great number of studies providing observations and assumptions about the activation behavior of TiFe alloy, the mystery of the activation mechanisms is still unsolved. The surface evolution and the hydrogen-alloy interaction during the activation processes are not well understood yet. More insightful research is still needed to reveal the universal rules of the activation behavior and mechanisms of TiFe alloys.

Extensive studies reported that the activation properties of TiFe alloys can be greatly improved by alloying with the third or multi-elements, adjusting Ti/Fe ratios, mechanical processes, and surface modification. The composition manipulating and mechanochemistry methods enabled the activation of TiFe-based alloys at room temperature [30,113]. The alloying method refers to the activation of TiFe alloys by addition with third or multi-elements, including transition metals, alkaline earth metals, rare-earth metals, p-block elements, and reactive non-metal elements [30]. Alternatively, adjusting the Ti/Fe atomic ratio of TiFe-based alloy is also effective in improving activation kinetics [114,115]. The surface modification including ion implantation [116] and catalytic layer deposition [117] also reported as the solutions for promoting the activation properties of TiFe alloys. There are also numerous attempts on improving the performance of TiFe by subjecting it to thermal or cold mechanical processing, although there is a lack of understanding of the effects of mechanical processing on the microstructure or compositions. The mechanical methods include cold pressing [118], high-energy ball milling [119,120], HPT [121], and cold rolling [122].

3. Synthesis methods

The hydrogen storage performance of TiFe alloy is strongly correlated with the microstructure, which is usually affected by synthesis methods. Most of the research on TiFe-based alloys is focused on the improvement of hydrogenation characteristics, especially activation properties. However, the development of cost-effective fabrication routes on the industrial scale is also considered critical for the practical application and commercialization of TiFe-based alloys. In general, traditional high-temperature melting of metallic elements under a controlled inert atmosphere with prolonged homogenization treatment is applied to fabricate TiFe alloys. The predominant traditional casting methods are time- and energy-intensive processes since they are usually melted at a high temperature for well-mixing. As a result, the emergence of novel and economical synthesis methods for TiFe-based alloys and their derivatives has become an increasingly exciting topic in recent decades [29,31,123]. Versatile techniques have been utilized to synthesize TiFe-based alloys, including mechanical alloying, combustion synthesis, electro-deoxidation, solid-state thermochemical reactions, physical vapor deposition, high-pressure torsion (HPT), and gas atomization.

3.1. Casting

Casting methods are generally used in TiFe-based hydrogen storage alloys involving arc melting and induction melting, among which, arc melting is a traditional method to prepare TiFe-based alloys. Reilly et al. [54] first introduced arc-melted TiFe alloy for hydrogen storage. Up to now, arc melting is still extensively employed for the preparation of TiFe-based alloys for hydrogen storage, due to the advantage of high scalability and ease of operation. Recently, Shang et al. [124] developed the method for synthesizing TiFe alloy from industrial scraps of iron (steels C45 and 316 L) and titanium (Ti alloy Grade 2), the as-melted alloys can absorb a maximum amount of hydrogen of 1.61 wt% and 1.50 wt% at 50 °C and a pressure of 0 to 100 bar. Compared with arc melting, induction melting was mostly employed for the preparation of TiFe alloys with volatile elements (La, Mg, Y, Ni, Mn, etc.). Dematteis et al. [73] reported Ti-Fe-Mn ternary alloys by induction melting followed by annealing and quenching. The as-prepared $TiFe_{0.85}Mn_{0.05}$ alloy obtained 1.73 wt% of hydrogen capacity, and it can be activated at 25°C under 2.5 MPa of hydrogen [73]. More recently, Barale et al. [125] investigated $TiFe_{0.85}Mn_{0.05}$ alloy for a hydrogen storage plant by induction melting. A 5 kg batch of alloy obtained a hydrogen storage capacity is of 1.0 H_2 wt% at 55 °C and the sorption properties maintained over 250 cycles [125]. Overall, casting is considered a convenient and mature method for the synthesis of TiFe-based alloys.

3.2. Mechanical alloying

Mechanical alloying is an efficient way to produce nanocrystalline TiFe alloy and to introduce interfaces and defects in materials [126], which are helpful for the initial hydrogenation kinetics. Zaluski et al. [127] discovered that the crystallization state of TiFe produced by ball milling is determined by the oxygen content. Higher oxygen content (higher than 2.9 at.%) leads to the formation of an amorphous alloy. Morris et al. [128] found that the mechanical alloying of TiFe alloy considerably facilitates the reaction with hydrogen. The mechanical alloyed TiFe can be activated at thermal cycling up to 300 °C in the hydrogen atmosphere [128]. Nanocrystalline TiFe showed enhanced absorption and desorption kinetics, even at relatively low temperatures [128]. The improvement in activation by mechanical alloying is believed to be attributed to the availability of well-established diffusion paths for hydrogen atoms and hydrogen atoms preferentially dissolving into the inter-grain region [129].

Despite the mechanical alloyed TiFe alloys can be activated at lower temperatures and even without the hydrogen, it may also result in amorphization of the compound and disappearance of the plateau at pressure-composition isotherms, which significantly reduce the hydrogen storage capacity [127,130]. Therefore, the post heat treatment of ball-milled TiFe had been developed for the recrystallization of amorphous TiFe to restore the initial material hydrogenation ability. Abe et al. [131] found that the 10 h and 40 h milled TiFe alloys can absorb hydrogen readily after heat treatment at 300 °C for 3 h. Hotta et al. [132] reported that 20 h ball-milled TiFe alloy exhibited a maximum hydrogen capacity of 1.3 wt% at 25 °C, after heat treatment at 300 °C in the vacuum and 15 MPa in a hydrogen atmosphere five times repeatedly. Zadorozhnyy et al. [133] discovered that the ball milling synthesized TiFe alloy has a room temperature hydrogen capacity of about 1.4 wt%. The activation of the alloy is completed by vacuum degassing the alloy and heating under hydrogen at a pressure of 1 MPa and a temperature of 400 °C for 30 min [133]. Generally, the mechanical alloyed TiFe still requires thermal activation cycles at hydrogen pressure or vacuum for the first absorption.

Moreover, the yield of mechanical alloying of TiFe alloy is also a significant concern, due to the welding of the powders to the milling media. Abe et al. [131] utilized 5 h mechanical alloying because the collection efficiency of sample powder is relatively good (over 85%). Falcao et al. [134] performed the mechanical alloying of TiFe using different organic Process Control Agents (PCAs), such as ethanol, stearic acid, low-density polyethylene, benzene, and cyclohexane. Cold welding can be controlled by the addition of PCAs (10 wt% or over) and replacing Ti with fragile TiH_2, the as-produced TiFe exhibit yields ranging from 90–95 wt% [134]. After post-heating milled samples at 873 K under vacuum, the alloy exhibited a maximum hydrogen capacity of 0.94 wt% at room temperature [134]. More recently, Vega et al. [135] propose a method by using a pre-milled vessel with stearic acid as PCAs. Nanocrystalline TiFe was synthesized in this way with low oxygen contamination, and full yields for milling time of 6 h or longer, requiring no heat treatments for the first hydrogen absorption [135]. The hydrogen storage capacity of 1.0 wt% at room temperature under 20 bar was attained by the sample milled for 6 h [135].

An alternative mechanical alloying method to produce TiFe alloy is HPT. The HPT process became popular not only for processing but also for synthesizing various kinds of hydrogen storage materials [136]. Recently, López-Gómez et al. [137] reported nanostructured TiFe synthesized by mechanical alloying via HPT. After activation treatment by a single-cycle evacuation at 673 K for 2 h, the as-synthesized TiFe could absorb hydrogen of ~1.4 wt% at room temperature [137]. Nonetheless, research regarding the synthesis of TiFe alloy by HPT is still rare.

3.3. Chemical synthesis from ore or mixed oxides

To minimize the energy consumption and avoid using pure metallic Ti, the combustion synthesis, electro-deoxidation, and chemical synthesis were also developed based on using Ti oxide (TiO_2), $TiFeO_3$, ilmenite, or even $Fe(NO_3)_2{\cdot}6H_2O$.

Combustion synthesis is one of the techniques that has attracted considerable attention. In 2005, Wu et al. [138] proposed the combustion synthesis of TiF powder and the magnesiothermic reduction of ilmenite. After leaching by hydrochloric acid, the product is composed of TiFe, $TiFe_2$, and a few other intermediate phases [138]. Later, Tsuchiya et al. [139] developed the combustion synthesis of a TiFe-based hydrogen storage alloy from Fe and TiO_2 using metallic calcium as the reducing agent and heat source. The TiFe powders produced by combustion synthesis exhibit around 8 mm in size and 1.39 wt% of hydrogen storage capacity at 298 K [139]. More recently, Deguchi et al. [140] produced TiFe alloy through combustion synthesis by utilizing the magnesiothermic reduction reaction. The TiFe synthesized in a pressurized hydrogen atmosphere exhibited 1.06 wt% of hydrogen capacities and flat plateaus. Wakabayashi et al. [141,142] synthesized various types of TiFe-based alloys by self-ignition combustion synthesis (SICS) using Fe and Ti fine powders. In this method, well-mixed raw materials in the desired molar ratio were uniformly heated up to the ignition point in a pressurized hydrogen atmosphere, the product was synthesized with the help of the exothermic reaction of titanium hydrogenation [141,142]. Saita et al. [143] produced α-hydride of TiFe using Ti as a heat supply by hydriding combustion synthesis (HSC). After activation treatment by evacuating the product and charging hydrogen on the product at a temperature of 400 °C, the product stored hydrogen of 1.7 wt% at 25 °C [143].

Electro deoxidation can be applied for the extraction of Ti and also can be utilized for the synthesis of TiFe alloy. In 2006, Ma et al. [144] first introduced a direct electroextraction method of $TiFe_{0.4}Ni_{0.6}$ alloy powder from ilmenite with 0.85H/M of capacity at 25 °C. Tan et al. [145] synthesized TiFe from Fe_2O_3 and TiO_2 mixed and sintered oxide precursors. The electrolysis process yields TiFe, as well as Fe_2TiO_5 and TiO_2. Panigrahi et al. [146] explored the production of Fe—Ti alloy from mixed ilmenite and TiO_2 by a direct electrochemical reduction in molten $CaCl_2$. The mixed solid oxides were reduced to TiFe and $TiFe_2$ composite. Shi et al. [147] successfully fabricated the TiFe by the electrolysis of ilmenite at 900 °C. They further claimed that the increase in temperature promotes the mutual diffusion process, and it is favorable for the formation of TiFe alloy [148,149]. Xiong et al. [150] investigated the preparation of TiFe from ilmenite by the electrochemical reduction in $CaCl_2$-NaCl molten salt with CaO addition. It was found that 1 mol% CaO addition significantly improves the reduction rate of ilmenite [150]. Wang et al. [151] reported that TiFe alloy containing 16% β-Ti (Ti_4Fe) can be prepared from the mixed titanium-containing waste slag and Fe_2O_3 by electrolysis. More recently, Padhee et al. [152] studied the electro-deoxidation process for producing TiFe from low-grade ilmenite. The electro-deoxidation of TiO_2 and ilmenite mixed oxide pellet yielded a single-phase TiFe material [152].

Low temperature chemical synthesis is also proposed as a cost-effective method for the production of TiFe. Davids et al. [153] introduced the synthesis of TiFe–based alloy from mixed ilmenite and $FeTiO_3$ by a two-stage reduction using H_2 and CaH_2 as reducing agents. The as-prepared TiFe-based material achieved about 0.5 wt% of hydrogen capacity, the low capacity is due to the high amount of residual oxygen present in the alloy [153]. Kobayashi et al. [154,155] reported the fabrication of nano-structured TiFe from Ti—Fe oxide precursors (TiO_2 and $Fe(NO_3)_2{\cdot}6H_2O$ or commercial $FeTiO_3$ bulk powder) using a CaH_2 reducing agent in molten LiCl at as low as 600 °C. The 44–65 nm TiFe nanoparticles were obtained by this method. The as-synthesized alloy achieves a hydrogen capacity of 0.67 wt% [155].

These methods are feasible ways for the fabrication of TiFe-based alloys. However, activation at elevated temperatures is still generally required for the as-produced alloys. Moreover, the hydrogen sorption capacities strongly depend on the depletion of the oxygen from the raw materials to the formation of the alloys. The higher the oxygen content, the lower the hydrogen sorption capacities. The oxygen control in the final product is critical in the chemical synthesis processes.

3.4. Solid-state thermochemical reactions

Solid-state thermochemical reaction is also another promising method for the synthesis of TiFe. The Ti—Fe system is described by a phase diagram with several eutectics and intermetallic compounds. Heating the mixtures of Ti and Fe powders at a temperature above a eutectic point may be accompanied by contact melting [156]. Kivalo et al. [156] introduced the solid powder reaction route for the synthesis of TiFe alloy. It was found that sintering at 1100 and 1200 °C results in the formation of TiFe, the oxygen-containing compound Ti_4Fe_2O, and a small amount of Fe, but almost no trace of Ti [156]. Moreover, the appearance of the liquid phase during sintering was detected at the above eutectic temperature of 1085 °C [157]. Kivalo et al. [158,159] also investigated the effect of Mn on sintering processes in the Ti—Fe

system. It was discovered that the TiFe phase containing no Mn was formed at higher heating rates of Ti-Fe-Mn compacts, however, the phase of TiFe alloyed with Mn was formed at lower heating rates [158,159]. Antonova et al. [160] introduced the hydrogen atmosphere for the annealing compacts from mixtures of Ti and Fe. During hydrogen sintering at 1180 °C, the TiFe phase with a very small amount of $TiFe_2$ secondary phase was formed [160].

3.5. Physical vapor deposition

Physical vapor deposition (PVD) refers to those vacuum deposition processes in which the coating material is evaporated under vacuum by various mechanisms [161]. The PVD coating process is typically carried out between 100 and 600 °C, which is a unique production technique that can overcomes the limitations of melting processing [128,161]. For example, alloys that are impossible to produce by other techniques can readily be produced by PVD, including supersaturated compositions and ultra-fine microstructures [128]. Morris et al. [128] discovered that the TiFe alloy prepared by PVD with an electron beam was easier to be activated than commercial TiFe alloy. The as-synthesized alloy exhibited 1.2 wt% of hydrogen capacity [128]. Besides using an electron beam for PVD, pulsed ion beam evaporation is also utilized in the preparation of TiFe alloy [162,163]. By using Ti-40 at.% Fe targets, and crystallized Ti—Fe thin films without secondary phases were successfully obtained [162,163]. However, when using Ti-50 at.% Fe targets, β-Ti and $TiFe_2$ were observed along with the TiFe main phase [162,163]. Recently, Razafindramanana et al. [164] employed magnetron sputtering to synthesize TiFe/Zr/Pd tri-layers. With a total power of 80 W, TiFe layer with CsCl structure was obtained, followed by a Zr layer, and topped with a Pd layer. It was believed that the Zr and Pd layer protects against oxidation and provides dissociation of molecular hydrogen [164].

3.6. Gas atomization

Gas atomization is a promising synthesis process that can directly produce metallic powders at an industrial scale [165]. Alloys produced by gas atomization can achieve a cooling rate between 10^4 and 10^6 K/s, and thus enabled a fine microstructure [166,167]. For TiFe-based alloys, the fine secondary phase formation and its homogeneous distribution in the base TiFe matrix promote the hydrogen sorption kinetics [168]. Ulate-Kolitsky et al. [165] investigated the hydrogenation behavior of atomized TiFe-based alloys. In the gas-atomized powders, the TiFe-matrix was surrounded by finely distributed secondary phases. After activation by cold rolling for 1 and 5 passes, the TiFe+2 wt% Mn and 4 wt% Zr alloy reached a capacity of 2.1 wt% at room temperature [165]. Park et al. [169] reported the hydrogenation properties of a $TiFe_{0.85}Cr_{0.15}$ alloy prepared by gas atomization. The as-synthesized $TiFe_{0.85}Cr_{0.15}$ alloy achieved 1.34 wt% of hydrogen capacity under 40 bar H_2 at 30°C. More recently, Lee et al. [168] found that $TiFe_{0.8}Mn_{0.2}$ alloy prepared by gas atomization exhibits better hydrogenation kinetics than melted and crushed alloy ingots. It was believed that the extremely high cooling rate involved in gas atomization induced microstructural refinement and promoted the formation of secondary phases [168].

3.7. Synthesis methods and hydrogen storage properties

The characteristics and the effectiveness of different synthesis methods are compared in Table 3. Most of the fabrication methods of TiFe-based alloys still employ pure Ti and pure Fe as raw materials. However, for reducing the cost of the alloy preparation, there are also novel methods that utilize TiO_2 as the source of the Ti of the alloys. In addition, most of the synthesis process are completed in the oxygen free atmosphere such as under argon or hydrogen, so as to avoid surface contamination of the alloy. Nonetheless, the binary TiFe alloy synthesized by different methods still generally require a high activation temperature above 300°C. It is noted that the TiFe alloy fabricated by arc melting exhibits higher hydrogen capacity than the alloy that obtained by other techniques. Regardless of activation temperature, the best-performing material considering the hydrogen storage capacity is still the arc-melted material.

4. Activation properties and strategies

4.1. Effects of alloy compositions on activation properties

4.1.1. Ti/Fe ratios

Ti/Fe ratios greatly affected the activation behavior of TiFe-based alloys. Compared to the poor activation properties of TiFe, the initial

Table 3
The hydrogen storage properties of TiFe-based alloys prepared by different methods.

Synthesis methods		Alloy composition	Raw materials	Atmosphere	Maximum H_2 capacity	Desorption equilibrium pressure (bar), temperature (°C)	Activation Temperature (°C)	Ref
Casting	Arc melting	TiFe	Zone-refined Fe, Ti	Argon	1.9 wt%	5.2, 30	400–450	[54]
	Induction melting	TiFe	Ti, Fe	Argon	1.69 wt%	3.7, 25	400	[73]
Mechanical alloying	Ball milling	TiFe	Ti, Fe	Argon	1.4 wt%	6, 22	400	[133]
	High-pressure torsion (HPT)	TiFe	Ti, Fe	Air	~1.4 wt%	–	400	[137]
Chemical synthesis	Combustion synthesis + Magnesiothermic reduction	TiFe	TiO_2, Fe, Mg	Hydrogen	1.06 wt%	~1.5, 25	400	[140]
	Combustion synthesis + Calciothermic reduction	TiFe	TiO_2, Fe, Ca	Argon	1.39 wt%	~4, 25	300	[139]
	Hydriding combustion synthesis (HCS)	α-$TiFeH_{0.06}$	Ti, Fe	Hydrogen	1.7 wt%	–	400	[143]
	Self-ignition combustion synthesis	α-$TiFeH_{0.06}$	Ti, Fe	Hydrogen	1.55 wt%	–	25	[142]
	Low temperature chemical synthesis	TiFe	$Fe(NO_3)_2{\cdot}6H_2O$, TiO_2, CaH_2, LiCl	Hydrogen	~0.67 wt%	–	400	[155]
Solid-state thermochemical reactions		TiFe	TiH_2, Fe	Hydrogen	1.68 wt%	3.3, 23.5	450	[71]
Physical Vapor Deposition	Magnetron sputtering	TiFe/Zr/Pd	Ti, Fe, Zr, Pd	Argon	–	–	–	[164]
Gas atomization		TiFe+2 wt% Mn + 4 wt% Zr	Industrial grade Fe, Ti, Zr 702, electrolytic Mn	Argon	–	–	–	[165]

hydrogen absorption of $TiFe_{0.9}$ alloy can be easily achieved under moderate hydrogen pressures without the need for any thermal treatment. Lee et al. [115] found that the high Ti/Fe ratios of the of $Ti_{1+x}Fe$ ($0.1 \leq x \leq 0.5$) alloys prompted the formation of β-Ti. The β-Ti hydrogenated before the hydrogen absorption of TiFe, and the large volume expansion of β-Ti during hydrogenation caused the cracking TiFe matrix. The fresh surfaces exposed by cracking facilitate hydrogen interaction with TiFe. However, the roles of β-Ti can be questioned. Similar to TiFe, β-Ti is also easily oxidized with a passivating surface layer due to high oxygen affinity. And β-Ti is unable to absorb hydrogen at room temperature.

Guéguen et al. [75] and Dematteis et al. [73,78] also reported that the $TiFe_{0.9}$ alloy can be easily activated at 25 °C under hydrogen of 2.5 MPa. Despite the similar activation properties, the phase compositions of the $TiFe_{0.9}$ alloy are different. The induction-melted $TiFe_{0.9}$ alloy is composed of TiFe, β-Ti, and Ti_4Fe_2O phases [73,75,78]. It is suggested that the key parameter for the alloy activation is the density of interfaces between TiFe and secondary phases, instead of the β-Ti content of the alloy [78]. Park et al. [170] investigated the microstructure and surface oxide of $Ti_{1.2}Fe$ alloy. The $Ti_{1.2}Fe$ alloy requires no thermal activation process for the first hydrogenation, as shown in Fig. 6. It was claimed that the improved activation properties are due to the improved Ti concentration of the surface oxide layer [170].

These investigations suggest that the phase compositions of TiFe alloy with excessive Ti could vary depending on the synthesis methods and treatment conditions. But the significant improvement in activation properties by higher Ti/Fe ratios has been corroborated. The enhanced activation properties are ascribed to the effect of secondary phases.

4.1.2. Alloying

Alloying TiFe with one or multiple alloying elements is another method for tuning the activation kinetics, thermodynamics, cycle stability, and capacities. A large number of alloying elements for TiFe alloys were reported, including transition metals, alkaline earth metals, rare-earth metals, p-block elements, and reactive non-metal elements [30].

Alloying with transition metals is the most popular strategy for improving the activation kinetics of TiFe alloys. Numerous studies have been reported for using Mn [158,171,172], Zr [173,174], V [75,175], Cr [176,177], Co [178,179], Ni [180–183], Cu [176,184], Nb [185], Mo [186], Hf [187] and Ta [186] as alloying elements. The most extensively studied alloying element of TiFe alloy is Mn. The Mn substitution for Fe

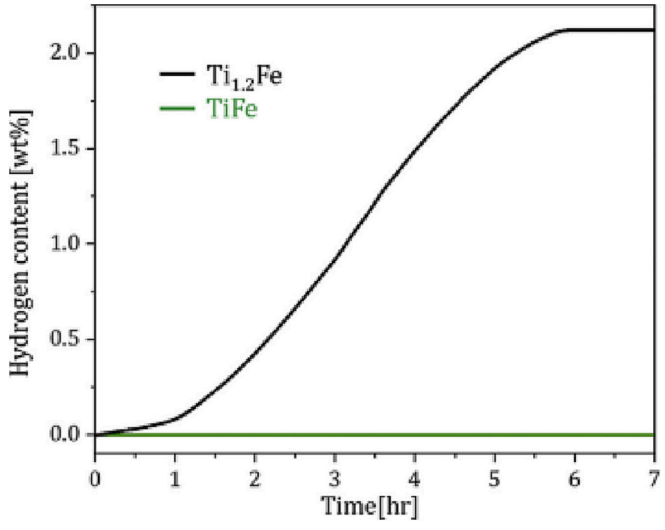

Fig. 6. Initial hydrogen absorption curves of the unactivated $Ti_{1.2}Fe$ and TiFe alloys at 25 °C and 40 bar of H_2. (Reprinted with permission from ref. [170]. Copyright 2021 Elsevier).

of TiFe alloy can improve activation kinetics, lower hydrogen sorption pressures, reduce hydrogen sorption hysteresis, increase hydrogen capacities, and promote long-term cycling performance [30]. Dematteis et al. [73] studied hydrogen storage properties of Mn alloying with Ti-rich TiFe alloys. The $TiFe_{0.85}Mn_{0.05}$ alloy is easily activated at 25 °C under 2.5 MPa of hydrogen. The alloy exhibit 1.73 wt% of hydrogen capacity [73]. Zr served as the substituent of Ti of TiFe alloys, it can greatly improve the activation kinetics and anti-poisoning stability. Jain et al. [181] reported the first hydrogenation of TiFe + 4 wt% Zr alloy exhibited 1.6 wt% of capacity, which was achieved at 40 °C under 2 MPa of hydrogen. The air-exposed Ti-Fe-Zr alloy can be activated at the same condition, but a 0.3 wt% loss in hydrogen storage capacity was observed [181]. The V addition to TiFe alloy facilitates the activation kinetics and improves the hydrogen capacity. $TiFe_{0.9}V_{0.1}$ alloy can be activated at 25 °C with a maximum capacity of 1.96 wt% [75].

Kumar et al. [82] studied hydrogen adsorption over the TiFe surface and doped TiFe by DFT calculations. It was revealed that 3-d metals substitution leads to the substitution of the surface Fe and Ti atom, and thus, enhanced hydrogen adsorption of TiFe. Among the 3-d transition metal atoms from Sc to Zn, partial substitution of TiFe surface atoms with V and Co will significantly enhance the hydrogen adsorption of TiFe [82]. Ko et al. [68] also explored the role of various alloying elements on the performance of stationary TiFe-based hydrogen storage alloys based on extensive DFT calculations. The grain boundary embrittlement is considered a possible way for enhancing the activation of hydrogen storage alloys because it can provide fresh surface regions without oxidation through the fracture of initial hydrogen storage alloys with surface oxides [68]. It was demonstrated that ternary alloying elements (such as La, Ce, Y, etc.) in TiFe alloys can cause grain boundary embrittlement [68].

Almost all the third element alloying with TiFe can improve the activation kinetics of TiFe alloy. However, the large amount of alloying elements addition will diminish the hydrogen capacity. This is due to the high-content elements alloying reducing the fraction of TiFe main phase of the alloy and promoting the content of the secondary phases. These secondary phases are usually unable to reversibly absorb/desorb hydrogen at ambient conditions [188,189]. Nonetheless, these secondary phases were reported as the pathway for the initial hydrogen absorption of the passivated TiFe-based alloys [190]. Recently, Ha et al. [191] suggested that the γ-Ce particles were dispersed in the TiFe matrix of TiFe alloys with V and Ce addition, which absorbed hydrogen prior to the hydrogenation of TiFe matrix. The Ce particles were hydrogenated into ε-CeH_2, initiating small cracks around the particles owing to the volume expansion of the hydride formation [191]. These cracks provided fresh surfaces for the subsequent hydrogenation of the TiFe matrix, and thus facilitated the activation of the alloy, as illustrated in Fig. 7.

Owing to good activation properties obtained by single element alloying of TiFe alloy, multi-element alloying with TiFe alloy was also extensively investigated to achieve a good combination of different aspects of hydrogen storage properties, such as hydrogen capacities, anti-poisoning ability, hydrogen sorption hysteresis, and plateau slope. For example, Patel et al. [192] found the combination of Zr and Mn addition to TiFe alloy exhibits significantly better hydrogen storage properties than the sole addition of Zr or Mn. The TiFe with 2 wt% Mn and 4 wt% Zr addition initially absorbed 2 wt% of hydrogen at room temperature under 2 MPa of hydrogen pressure, while TiFe +4 wt% Zr alloy only absorbed 1.2 wt% of hydrogen at the same condition [192]. Shen et al. [193] found the mischmetal addition to the $TiFe_{0.86}Mn_{0.07}Co_{0.07}$ alloy effectively enhances the cyclic stability properties in impure hydrogen gas containing oxygen. The hydrogen absorption capacity of $TiFe_{0.86}Mn_{0.07}Co_{0.07}$ + 4% Mm reaches 1.76 wt% at 25 °C [193]. Guéguen et al. [75] reported the addition of V to $TiFe_{0.8}Mn_{0.1}$ reduced the hydrogen sorption hysteresis and flattened the hydrogen sorption plateaus, meanwhile, the alloy maintained good activation properties at room temperature.

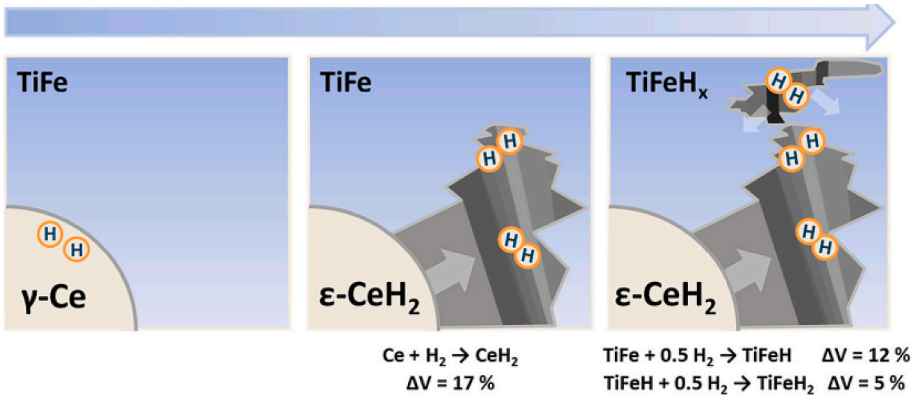

Fig. 7. Schematic illustration of secondary phases during initial hydrogen absorption of TiFe-based alloys. (Reprinted with permission from ref. [191]. Copyright 2023 Elsevier).

4.2. *Effects of mechanical processing on the activation*

Mechanical processes such as cold pressing, ball milling, HPT, and cold rolling have been used for the modification of hydrogen storage materials. These processes can introduce a non-equilibrium phase, nanoscale structure, and active sites such as defect or grain boundaries that can facilitate the hydrogenation kinetics [194]. For TiFe-based alloys, the activation kinetics can be effectively improved by these mechanical processes.

4.2.1. *Cold pressing*

Cold pressing employed for the activation of TiFe alloy was introduced by Bratanich et al. [195] in 1995. They found that the TiFe alloy pressed at 450 MPa was more easily activated than loose TiFe powders. Under 6 MPa of hydrogen, the complete activation of the loose TiFe powder was achieved at 623 K, while the TiFe compact was activated at ~373 K. They assumed that the improved activation behavior is due to the formation of fresh surfaces in the course of pressing, and these surfaces were protected from oxidation with contacts [195]. Later in 1996, they reported additional data that showed coarse TiFe particles (0.4–0.6 and 1.0–l.6 mm) could be activated at room temperature under a hydrogen pressure of 6 MPa without preliminary thermal and vacuum activation [118]. In contrast, the mechanical activation of TiFe samples from fine powders is not effective, as the hydrogenation processes are suppressed by oxidation. They believe the mechanical activation method for the interaction of intermetallic compounds with hydrogen through cold pressing of the powder sorbents, causes the brittle particles to break so that fresh surfaces are formed. However, the fine powder is oxidized more intensively than the coarse one [195].

4.2.2. *Ball milling*

As the mechanical alloying method, high energy ball milling involving repeated welding, fracturing, and rewelding of powder particles [126]. Ball milling was used as a method for the synthesis of TiFe-based alloys as well as a mechanical treatment method to overcome the activation barrier. Zaluski et al. [196] investigated the effect of ball milling on TiFe that was previously alloyed by arc melting and found that ball milling of TiFe leads to a refinement of the TiFe grains and chemical disordering of the material. Haraki et al. [197] studied the hydrogen storage properties of the melted TiFe after 2 h of ball milling. The milled TiFe powders were easily activated at 298 K and obtained a hydrogen storage capacity of 1.7H/FeTi. Emami et al. [119] reported that a crushed TiFe ingot could be effectively activated after processing by ball milling, the 36 h-milled TiFe alloys can absorb hydrogen up to 1.5 wt% of hydrogen at 303 K. They further claimed that ball-milled TiFe powder is not deactivated after being kept under air for ~1 month [119], which is remarkable if true, but we cannot find additional publications that repeat or verify the results. By using TEM, they found that the processing of TiFe using ball milling results in the formation of nanograins, while few cracks or dislocations are generated, and they believed the nanograin boundaries act as pathways for the transportation of hydrogen atoms through the oxide layer in the case of ball-milled TiFe, while the oxygen molecules cannot penetrate through these ultrafine pathways [119].

Based on ball milling, wet milling is also proposed for the activation of TiFe. Guo et al. [120]explored the activation behavior of TiFe alloys processed by wet milling with ethanol and hexane. The pre-alloyed TiFe powders milled with ethanol were found capable of absorbing 1.2 wt% of hydrogen at room temperature. It indicated that the addition of ethanol helped TiFe alloys to spread more easily during the milling process and reduce the oxidation layer easily, due to the higher polarity and high reducing ability [120]. Besides wet milling, reactive milling is reported to be effective for the activation of TiFe. Chiang et al. [198] introduced reactive ball milling in hydrogen atmosphere for the activation of pre-melted TiFe alloy. With initial hydrogen pressure of reaction system varying from 0.5 to 0.6 MPa, TiFe absorbed hydrogen during the milling process [198]. Recently, Patel et al. [199] reported that the reactive ball milling of ad arc-melted and crushed TiFe ingot can facilitate hydrogen absorption at room temperature without any thermal treatment or evacuation. Furthermore, they discovered a self-shearing reactive milling behavior without using milling agents. After intense movement of the powder or even chunks of the alloy under hydrogen pressure without any additional grinding media, the as-processed TiFe can also be activated at room temperature [199]. It was believed that the wear of particles caused by the movements, results in the exposure of a fresh active alloy surface that is active enough to absorb hydrogen [199].

4.2.3. *High-pressure torsion and cold rolling*

The bulk ultrafine-grained and nanostructure with large densities of lattice defects of alloys can be produced by severe plastic deformation (SPD) techniques [200]. SPD induced by HPT is considered a feasible way to activate passivated TiFe alloy [136,201]. Edalati et al. [121] introduced HPT for the activation of TiFe alloy. The HPT-processed TiFe exhibits heterogeneous microstructures composed of nanograins, coarse-grains, amorphous-like phases, and disordered phases; and it is able to absorb 1.7 wt% of hydrogen at room temperature. They further claimed that HPT-processed TiFe fragmented powders are not deactivated even after storage for several hundred days in the air [105], for which we have not been able to find other publications to corroborate. Cold rolling was also proposed for the activation of TiFe alloys [202,203]. The activation properties of TiFe for hydrogen storage using groove rolling and HPT were compared by Edalati et al. [202]. It was discovered that the groove-rolled sample, with a sub-grain structure and high density of dislocations and cracks, can also absorb hydrogen up to 1.7 wt% [202]. However, there are also contradicting reports. For

instance, Lv et al. [204] reported that cold rolling has minimal effect on the first hydrogenation of TiFe + x wt% $ZrMn_2$ ($x = 2, 4, 8, 12$). The cold rolling only slightly eliminated the incubation time of the first hydrogen absorption of TiFe alloy. It was believed that the alloy composition and other microstructure features have a much bigger impact on the activation behavior than mechanical treatment [205,206].

Despite the inconsistency regarding the effect on activation, cold rolling is still extensively reported as the mechanical solution for the activation of TiFe. Vega et al. [122]found that TiFe can be easily mechanically activated by cold rolling under an inert atmosphere after 20 or 40 passes. The average storage capacity of the cold-rolled alloy is 1.4 wt% H_2 for the first absorption at room temperature. Manna et al. [207] found that cold rolling and ball milling processes enabled the activation of air-exposed TiFe + 4% Zr alloy. Around a 10% decrease in storage capacity has been observed after cold rolling while the storage capacity decreased by ~50% after ball milling. They further discovered that the 30 days air-exposed TiFe + 4 wt% Zr + 2 wt% Mn alloy could be successfully hydrogenated after ball milling and after cold rolling with some loss in hydrogen storage capacity [208]. In addition, the loss in storage capacity was also more significant after ball milling than after cold rolling [208]. Lv et al. [205,206] demonstrated that cold rolling can effectively improve the activation kinetics of arc-melted TiFe + x wt% (Zr + 2 V) (x = 0, 4, 5, and 6) and TiFe + 12 wt% (Zr + 2Cr) alloys. Recently, Oliveira et al. [209] reported that cold rolling was successful in activating the cold-rolled pre-alloyed TiFe that were prone to absorb hydrogen without additional thermal treatments. The samples exhibited fast hydrogenation/dehydrogenation kinetics, mainly attributed to the cracks on the surface of powder particles and refined grain sizes. Absorption/desorption capacities reached approximately 1.1 and 0.7 wt% hydrogen, respectively. Similar observations are reported in the work of Ulate-Kolitsky et al. [165]. The TiFe + 2 wt% Mn and 4 wt% Zr alloy prepared by gas atomization can be activated by cold rolling for 1 and 5 passes and reaching a capacity of 2.1 wt% at room temperature [165].

As a summary of the mechanical activation methods, the common theme was to break the surface oxide layer and create fresh surfaces to facilitate hydrogenation. The defects in the material after mechanical treatment may also have played a role. However, the claims about the material can still hydrogenate after long-term exposure to the air is inconsistent with the explanation based on the surface oxide layer. These materials will form new oxide layers during exposure to the air. If the crystalline defects are responsible for better activation kinetics, such an effect may diminish during cycling. It should be important to demonstrate the ability of these materials through de/hydrogenation cycling.

4.3. Effects of surface modification on the activation

Apart from the approaches and techniques mentioned above, surface modification is also employed for enabling the activation of TiFe alloy. In 2002, Suda et al. [116] introduced ion implantation to modify the surface of the TiFe alloy for the improvement of initial activation properties. They found that the argon-ion mixing caused extensive improvement of initial activation, wherein hydrogenation was easily achieved at 373 K and 1 MPa. Heller et al. [210] studied the kinetics of hydrogen uptake of thin films of TiFe deposited on Si substrates and covered with 20 nm Pd. They found that the TiFe/Pd films exhibit fast hydrogen absorption kinetics without the need for thermal treatment [210]. Williams et al. [117] investigated surface modification of the sintered $Ti_{1.1}Fe_{0.9}O_x$ and arc-melted TiFe using autocatalytic deposition of the Pd-based catalytic layers to achieve improvement of the H storage characteristics. It was confirmed that Pd deposition is efficient in significant facilitation of the hydrogenation ability of the materials at moderate H_2 pressures and room temperature [117]. Davids et al. [211] utilized a metal-organic chemical vapor deposition technique (MOCVD) to achieve surface modification of TiFe alloy. During this process, the thermal decomposition of palladium (II) acetylacetonate ($Pd[acac]_2$) is mixed with the powder of the parent TiFe alloy. It was found that surface modification of TiFe alloy by MOCVD of Pd using $Pd[acac]_2$ as a precursor resulted in the formation of coatings constituted by Pd nanoparticles which promote the hydrogenation ability of the material [211]. It was believed that the effect was associated with the improved catalytic activity of the modified surface towards the H_2 dissociation [211].

4.4. Activation strategies

Alloy composition engineering, mechanical treatment, and surface modification are all feasible methods for the activation of TiFe-based alloys. Among those activation strategies, modifying alloy compositions seems to be the best option for achieving a combination of good hydrogen storage capacity and moderate activation temperature as shown in Fig. 8. Fig. 8 also briefly compares the mechanically processed TiFe alloys, single and multi-element alloyed TiFe alloys with the untreated TiFe. It should be noted that TiFe alloyed with transition metals appears to exhibit the most promise for lowering activation temperature and maintaining a good hydrogen storage capacity.

5. Cycle stability and anti-poisoning ability

TiFe alloy has excellent cycle stability at low pressures when only the first plateau is involved. Johnson et al. [215] demonstrated that the TiFe alloy can be cycled under 32 to 34 bars of hydrogen for ~13,000 times at the temperature ranging from −7°C to +110°C without detectable deterioration. However, TiFe alloy that cycles at elevated pressures beyond the second plateau could experience a decrease in hydrogen storage capacity. Goodell et al. [72] observed an obvious increase in the second plateau pressure during the cycling of TiFe. The increase of γ-phase dihydride reaction pressure was found to reduce the hydrogen capacity in the test pressure range. Reilly et al. [216] also reported the disappearance of the upper plateau after 3011 hydrogen sorption cycles of TiFe alloy at 0°C and 65 bar pressure. The authors assumed the change in the PCT curve is due to lattice strain and associated defects produced in the alloy during cycling. Ahn et al. [217] also confirmed that the shapes of the PCT curves of TiFe change as a function of the number of thermal cycles. It was observed that the hydrogen storage capacity gradually decreases as the number of cycles increases due to the suppression of the γ-phase formation in the hydride after about 1000 thermal cycles [184]. The authors claimed that the degradation may associate with the formation of stable hydrides during thermal cycling, which impedes the occupation of interstitial sites for the γ-phase dihydride [217]. Besides binary TiFe alloy, the substituted TiFe alloy also exhibits good cycle stability. The $TiFe_{0.85}Mn_{0.15}$ alloy exhibited no loss in capacity after ~30,000 times back and forth hydrogen sorption cycling through a lower pressure plateau [218]. The $TiFe_{0.8}Ni_{0.2}$ alloy only presented 15% degradation in hydrogen capacity after 45,000 cycles in the temperature and the pressure ranges of 20 °C–185 °C and 0.5–9 bar, respectively [219]. It was found that the capacity decreases of $TiFe_{0.8}Ni_{0.2}$ alloy are due to the slight increase of the first absorption equilibrium pressure after long-term cycling [219].

TiFe alloy has poor anti-poisoning ability, the hydrogen storage properties of which could significantly degrade upon contact with gas impurities. Reilly et al. [220] reported that TiFe is very sensitive to the presence of oxygen, and the O_2 impurity in hydrogen can decrease hydrogen sorption capacity of TiFe. Sandrock et al. [221] found that the TiFe alloy cycling with O_2, CO, or H_2O-contaminated hydrogen exhibited a significant decrease in hydrogen sorption kinetics and effective capacities. The contamination of surfaces thus deactivates the TiFe alloy. The surface poisoning by these impurities was believed to inhibit the dissociation of hydrogen molecules and hydrogen penetration [221].

Alloying with other elements can effectively improve the anti-poisoning ability of TiFe alloy. Compared to binary TiFe alloy, the substituted TiFe alloy exhibits better resistance to impurity poisoning. The $TiFe_{0.85}Mn_{0.15}$ alloy is reported to have some resistance to capacity

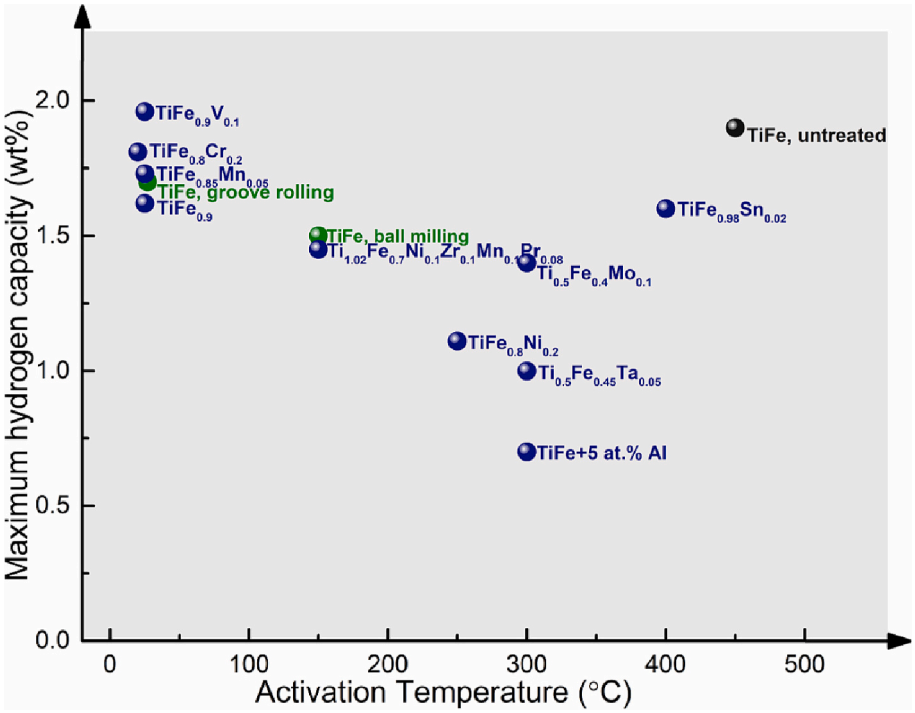

Fig. 8. Relative comparisons of the reported activation temperatures and hydrogen storage capacities of TiFe-based alloys [54,73,75,119,136,176,180,186,212–214].

loss when in contact with CO [221]. When cycling with CO-contaminated impure hydrogen, TiFe lost all hydrogen capacity rapidly, however, $TiFe_{0.85}Mn_{0.15}$ alloy could preserve a small level of effective capacity [221]. As mentioned earlier, the anti-poisoning ability of TiFe can be also improved by Zr alloying. The room temperature activation of air-exposed Ti-Fe-Zr alloys is reported [188,208]. Besides Zr and Mn, the addition of misch metal to TiFe-based alloys can also promote resistance to surface poisoning [87,193]. Despite the improvements by alloying with these elements, the long-term anti-poisoning ability needed to be further evaluated.

6. Applications

The attempts of the applications began right after the discovery of TiFe for hydrogen storage. In the 1970s, Brookhaven National Laboratory initiated the development of bulk storage techniques for hydrogen using TiFe alloy [222,223]. The program consisted of engineering analysis and design of a large bulk hydrogen storage facility, engineering-scale tests, work on the selection and development of suitable TiFe alloys, and the construction of a large prototype energy storage system [215,224]. In 1974, the first relatively large stationary hydrogen storage container using TiFe hydride was built for an electric peak shaving demonstration by the Public Service Electric & Gas (PSE&G) Company of New Jersey [225,226]. This container was 570 kg in weight and 0.144 m^3 in a volume filled in with 400 kg of TiFe alloy, and it could store up to 6.4 kg of H_2 under up to 37 atm of pressure [223,227]. In 1977, a 6-in.-diameter about 30-in. long hydrogen storage test bed was built [228]. The test bed contained ~38.55 kg of TiFe alloy with a maximum hydrogen storage capacity of 1.19 wt% and a uniform hydrogen flow rate of 9 standard liters per minute (0.32 SCFM) sustained for a 10-h transfer period [228]. Moreover, the techno-economic assessments were carried out for a hydrogen-chlorine (H_2-Cl_2) energy storage system for electric utility load leveling and peak shaving applications for using TiFe as hydrogen storage material [229,230]. The $TiFe_{0.85}Mn_{0.15}$ alloy was considered as optimum for the H_2-$C1_2$ unit [215,230,231].

The TiFe alloys were also considered for automobiles. Several hydrogen-powered vehicles were built using TiFe alloy as the fuel storage medium [223]. Two of these vehicles undergone extensive testing, a Winnebago bus which was converted to hydrogen fuel by the Billings Energy Corp. of Provo, Utah [232], and a small van built by Daimler Benz A, G. (now Mercedes Benz) of Suttgart [233]. For the Winnebago bus, it was believed that TiFe hydride can be used in transit vehicles because the necessary weight can be carried. The 19-passenger bus was found capable of 4 h of operation on an established service route [232]. Further, Billings also employed TiFe hydrides in a postal vehicle [234,235]. Daimler-Benz developed a hydrogen storage unit consisting of three modules which have an overall weight of about 365 kg with 280 kg of TiFe hydride, this unit can store 5.0 kg of hydrogen [236]. They also designed and out-fitted the TiFe hydrides in the delivery van, combined with high-temperature hydrides (Mg_2Ni) as storage units [236–239]. Beneito et al. [240] developed an electric toy vehicle powered by a fuel cell stack. The system consisted of a 150 W PEMFC stack powered by hydrogen/air, a tank of metal hydrides of TiFe alloy type with a capacity of 300 standard liters, for storing hydrogen, and an electronic power device based on electrolytic capacitors, to supply peak power demands during acceleration and start-up of the vehicle [240].

Despite the high volumetric energy density of TiFe, the low gravimetric hydrogen capacity limits its vehicular applications. The ultimate target for on-board hydrogen storage systems of the Department of Energy of the United States requires 6.5 wt% of hydrogen capacity [241]. While it is not suitable for onboard applications, TiFe is considered one of the prime candidates for stationary hydrogen storage. Uchida et al. [242] demonstrated a wind-solar hybrid energy storage system constructed to store electricity from wind and solar energy as hydrogen and to utilize the produced hydrogen for a fuel cell using nano-structured TiFe as hydrogen storage materials. Three hydrogen storage tanks were installed to absorb the hydrogen gas generated from the solid polymer electrolyte (SPE), each tank contained 900 g of the nano-structure TiFe alloy [242]. Endo et al. [243] studied the activation processes of a 55 kg TiFe-based alloy that was filled in a conventional bench-scale tank under 1.0 MPa Gauge and at 80 °C. They discovered

that, at a constant hydrogen flow rate of 20 NL/min (normal liters per minute), the TiFe-based tank absorbed and desorbed >8 Nm^3 hydrogen at inlet brine temperatures of 60 °C and 70 °C, respectively [243]. A bench-scale stationary hydrogen tank (80 Nm^3) using TiFe hydrides (520 kg) with a polymer electrolyte membrane (PEM) electrolyzer was incorporated for hydrogen production (5 Nm^3/h) and PEM fuel cells (FC) for hydrogen use (3.5 kW) [244], and the integrated system was operated under various weather conditions [245].

The optimization of design and parameters such as porosity, thermal conductivity, and strain variation of the TiFe hydride tank are also reported. Halıcıoğlu et al. [246] investigated the charging time and the role of the heat transfer mechanism by obtaining temperature histories which were measured at several points in the reactor. They found that the as-prepared reactor filled with 105 g TiFe-C powder exhibited a 0.44% hydrogen storage rate at a relatively low charging pressure of 12 bar. Duan et al. [247] studied the strain variation of a hydrogen storage tank packed TiFeMn alloy. It was found that plastic deformation occurred during the activation process which did not increase during the following ab-desorption cycles though the tank still had the ability for elastic deformation, the stress induced by the alloy swell on the tank was over 8 MPa [247]. More recently, Matsushita et al. [248] explored the porosity and effective thermal conductivity in a packed bed of nanostructured TiFe for use in hydrogen storage tanks. It was found that the total volume of the nanostructured TiFe-packed bed decreased with every passing cycle of expansion and contraction, and this reduced porosity is preferred for hydrogen storage tanks [248]. Moreover, the effective thermal conductivity of nanostructured TiFe changes from 0.4 to 1.1 W/mK according to reacted fraction rise and according porosity decrease [248].

Recently, there are some studies from Europe on the development of TiFe-based alloys for stationary hydrogen storage. The materials include TiFe-Mn [125], TiFe-Zr-Mn [165,192], and TiFe-Zr-Mn-V [249] alloys. Bellosta von Colbe et al. [250] studied scaled-up milling in a 100 L device for processing powder TiFeMn alloy from GKN and found that a TiFeMn alloy milled for just 10 min in a 100 L industrial milling device showed excellent hydrogen storage properties without any thermal treatment. Barale et al. [125] evaluated the hydrogen storage properties of $TiFe_{0.85}Mn_{0.05}$ alloy produced at the industrial level for a hydrogen storage plant. A batch of 5 kg of $TiFe_{0.85}Mn_{0.05}$ alloy was synthesized by induction melting, exhibiting the storage capacity of 1.0 wt% of H_2 at 55 °C, and the sorption properties are maintained over 250 cycles. The work was part of the EU-funded HyCARE (Hydrogen CArrier for Renewable Energy Storage) project [125]. This project aims to develop a prototype large-scale hydrogen storage tank using a solid-state hydrogen carrier based on metal powder, that will operate at low pressure and temperature [125]. The project involves the production of almost 5 tons of metal powder, which will be placed in special containers [125,251]. The aim is to store 50 kg of hydrogen, the highest quantity yet stored in Europe using this technique [218]. The $TiFe_{0.85}Mn_{0.05}$ alloy was selected as an H_2 carrier for this plant [125].

TiFe alloys can also be utilized as thermal energy storage materials [252,253]. The Australian EMC Solar company had developed a concept for a concentrated solar tower (CST) plant with a CaH_2-heat storage system and a Stirling engine with a continuous output of 100 kW_{el} [254]. The released hydrogen during the energy storage process is stored as TiFe hydride. Feng et al. [255] conducted a complete techno-economic analysis of screening the metal hydride pairs MgH_2&TiFeMn and MgH_2&LaNiAl. Based on the life cycle economic analysis, matching of MgH_2&TiFeMn is considered to be a better selection due to a smaller levelized thermal storage cost (28 USD/kWh_{th}), where two major expenses are the capital cost and energy consumption cost, which are 74.3% and 19.3% respectively [255]. Corgnale et al. [256] carried out a techno-economic assessment of destabilized Li hydride systems coupled with TiFe for high-temperature thermal energy storage. The storage system demonstrated excellent volumetric capacity, achieving values between 100 and 250 kWh_{th}/m^3 [256].

Apart from being applied as hydrogen storage media, TiFe-based alloys were also proposed as catalysts for the ammonia synthesis [257,258], CO_2 reductions [259,260], and de/hydrogenation of MgH_2 [261–263]. For instance, the room temperature hydrogen absorption of hydrogen can be facilitated by the catalytic effect of TiFe-based alloys [263]. The addition of binary TiFe alloy to the MgH_2 reduced the desorption temperature and significantly improved the hydrogen sorption kinetics of MgH_2 [262].

7. Summary and perspectives

TiFe-based alloys have shown great potential owing to their moderate operating temperature, high volumetric capacity, and low cost. The innovation and development of synthesis methods, activation mechanisms, activation strategies and applications are of great importance of TiFe-based alloys. The major hindrance to the application is the harsh conditions required for activation before reversible hydrogen sorption. The observations and assumptions based on the evolution of the surface oxide layer during activation treatment provide thoughtful insights, especially regarding the surface composition evolution and the role of secondary phase. Nonetheless, current studies of activation behavior still lack solid evidence for revealing the general mechanisms.

This review outlines various methods for preparing TiFe-based alloys. Owing to the ease of operation and scalability, the most adopted fabrication approach is still arc-melting. However, there is growing interest in developing low cost and low energy-consuming route using low-cost raw materials (oxides or ilmenite). TiFe-based alloys synthesized by novel processes should not only be cost-effective but also should possess desirable hydrogen storage properties.

The review evidenced that the activation properties can be significantly enhanced by compositional design, mechanical processing, and surface modification. The most prevailing strategy for the activation of TiFe is alloying with single or multi-elements. Thermal activation treatment can be eliminated for the initial hydrogenation of TiFe by alloying. Nonetheless, the addition of other elements to TiFe alloys generally results in a decrease in hydrogen capacity and lower sorption plateau pressure. The in-depth theoretical design of TiFe-based alloys for combining multiple aspects of hydrogen storage properties is scarce in the literature. More understanding of the alloy design is needed for optimizing compositions for better hydrogen storage properties. Also, the comprehensive assessments of hydrogen storage properties of TiFe-based alloys, including activation kinetics, thermodynamics, cycle stability, and anti-poisoning ability, need to be carried out for the selection of optimal materials.

The attempts for the applications from the 1970s to now indicate the huge potential of TiFe alloys for hydrogen storage. TiFe-based alloys can not only be utilized as a part of the thermal storage system, but more importantly, it has shown great prospects in stationary hydrogen storage applications for storing renewable electricity. The application of stationary hydrogen storage from renewable energy sources is illustrated in Fig. 9. The stationary hydrogen storage applications require a wide range of operation temperature (−40–50 °C) and rapid hydrogen sorption kinetics within 3 min [59]. In addition, more than 2 wt% of hydrogen storage capacity and less than 30% of capacity loss during 10,000 cycles are also needed [59]. The TiFe-based alloys generally satisfy the thermodynamic and kinetics requirement, but the capacity and long-term cycling stability still need to be improved when combining a good activation property. However, the relatively low cost of TiFe-based alloys compared to other hydrogen storage materials has prompted extensive ongoing research. With continuing development, it is likely the commercial-scale application for the TiFe-based alloys will be realized in the near future.

Declaration of competing interest

The authors declare that they have no known competing financial

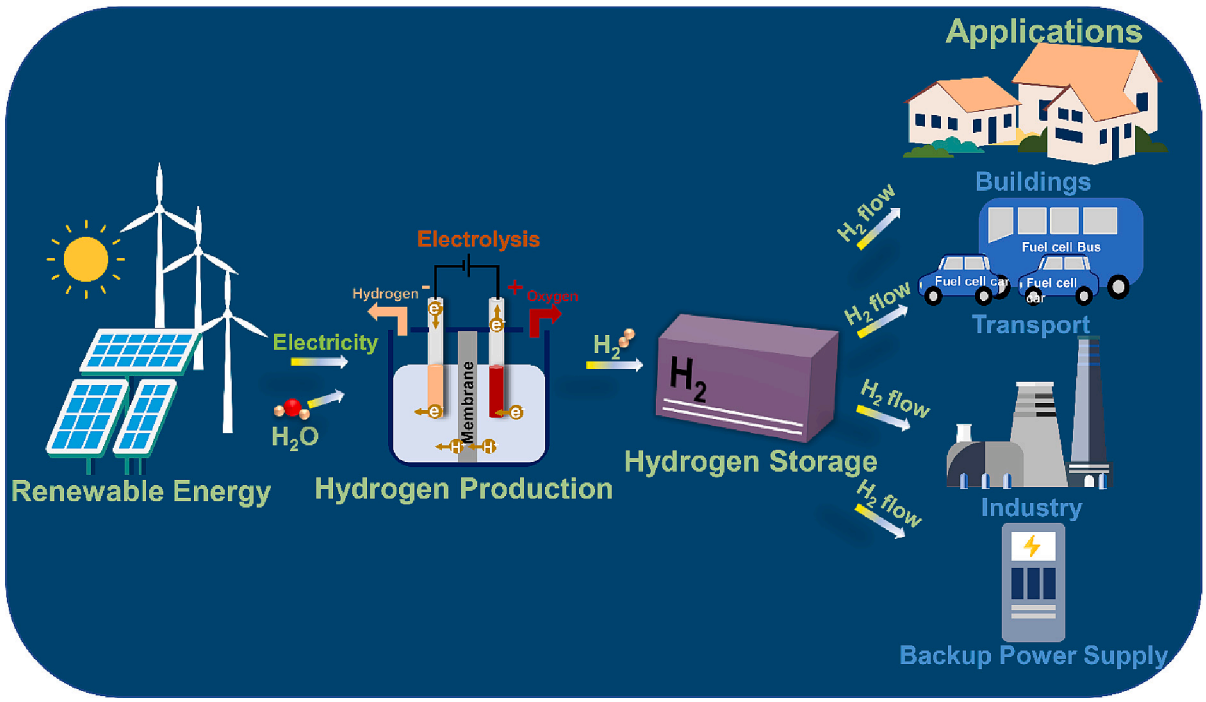

Fig. 9. Applications of stationary hydrogen storage from renewable energy sources.

interests or personal relationships that could have appeared to influence the work reported in this paper.

Data availability

Data will be made available on request.

Acknowledgments

The authors acknowledge the financial support for this work provided by Blacksand Technology LLC.

References

[1] I. Staffell, D. Scamman, A. Velazquez Abad, P. Balcombe, P.E. Dodds, P. Ekins, N. Shah, K.R. Ward, The role of hydrogen and fuel cells in the global energy system, Energy Environ. Sci. 12 (2) (2019) 463–491, https://doi.org/10.1039/C8EE01157E.

[2] A. Boretti, Hydrogen internal combustion engines to 2030, Int. J. Hydrog. Energy 45 (43) (2020) 23692–23703, https://doi.org/10.1016/j.ijhydene.2020.06.022.

[3] H.L. Yip, A. Srna, A.C.Y. Yuen, S. Kook, R.A. Taylor, G.H. Yeoh, P.R. Medwell, Q. N. Chan, A review of hydrogen direct injection for internal combustion engines: towards carbon-free combustion, Appl. Sci. 9 (22) (2019) 4842, https://doi.org/10.3390/app9224842.

[4] R.K. Mehra, H. Duan, R. Juknelevičius, F. Ma, J. Li, Progress in hydrogen enriched compressed natural gas (HCNG) internal combustion engines - a comprehensive review, Renew. Sust. Energ. Rev. 80 (2017) 1458–1498, https://doi.org/10.1016/j.rser.2017.05.061.

[5] J.O.M. Bockris, A hydrogen economy, Science 176 (4041) (1972) 1323, https://doi.org/10.1126/science.176.4041.1323.

[6] A.M. Oliveira, R.R. Beswick, Y. Yan, A green hydrogen economy for a renewable energy society, Curr. Opin. Chem. Eng. 33 (2021), 100701, https://doi.org/10.1016/j.coche.2021.100701.

[7] S. Niaz, T. Manzoor, A.H. Pandith, Hydrogen storage: materials, methods and perspectives, Renew. Sust. Energ. Rev. 50 (2015) 457–469, https://doi.org/10.1016/j.rser.2015.05.011.

[8] X. Yu, Z. Tang, D. Sun, L. Ouyang, M. Zhu, Recent advances and remaining challenges of nanostructured materials for hydrogen storage applications, Prog. Mater. Sci. 88 (2017) 1–48, https://doi.org/10.1016/j.pmatsci.2017.03.001.

[9] J. Huot, D.B. Ravnsbæk, J. Zhang, F. Cuevas, M. Latroche, T.R. Jensen, Mechanochemical synthesis of hydrogen storage materials, Prog. Mater. Sci. 58 (1) (2013) 30–75, https://doi.org/10.1016/j.pmatsci.2012.07.001.

[10] A. Züttel, Hydrogen storage methods, Naturwissenschaften 91 (4) (2004) 157–172, https://doi.org/10.1007/s00114-004-0516-x.

[11] J.O. Abe, A.P.I. Popoola, E. Ajenifuja, O.M. Popoola, Hydrogen energy, economy and storage: review and recommendation, Int. J. Hydrog. Energy 44 (29) (2019) 15072–15086, https://doi.org/10.1016/j.ijhydene.2019.04.068.

[12] H. Barthelemy, M. Weber, F. Barbier, Hydrogen storage: recent improvements and industrial perspectives, Int. J. Hydrog. Energy 42 (11) (2017) 7254–7262, https://doi.org/10.1016/j.ijhydene.2016.03.178.

[13] R. Moradi, K.M. Groth, Hydrogen storage and delivery: review of the state of the art technologies and risk and reliability analysis, Int. J. Hydrog. Energy 44 (23) (2019) 12254–12269, https://doi.org/10.1016/j.ijhydene.2019.03.041.

[14] P. Kowalczyk, R. Hołyst, M. Terrones, H. Terrones, Hydrogen storage in nanoporous carbon materials: myth and facts, Phys. Chem. Chem. Phys. 9 (15) (2007) 1786–1792, https://doi.org/10.1039/B618747A.

[15] S.J. Yang, H. Jung, T. Kim, C.R. Park, Recent advances in hydrogen storage technologies based on nanoporous carbon materials, Prog. Nat. Sci.: Mater. Int. 22 (6) (2012) 631–638, https://doi.org/10.1016/j.pnsc.2012.11.006.

[16] H.W. Langmi, J. Ren, B. North, M. Mathe, D. Bessarabov, Hydrogen storage in metal-organic frameworks: a review, Electrochim. Acta 128 (2014) 368–392, https://doi.org/10.1016/j.electacta.2013.10.190.

[17] J. Ren, H.W. Langmi, B.C. North, M. Mathe, Review on processing of metal–organic framework (MOF) materials towards system integration for hydrogen storage, Int. J. Energy Res. 39 (5) (2015) 607–620, https://doi.org/10.1002/er.3255.

[18] S.S. Han, H. Furukawa, O.M. Yaghi, W.A. Goddard III, Covalent organic frameworks as exceptional hydrogen storage materials, J. Am. Chem. Soc. 130 (35) (2008) 11580–11581, https://doi.org/10.1021/ja803247y.

[19] S.S. Han, J.L. Mendoza-Cortés, W.A. Goddard Iii, Recent advances on simulation and theory of hydrogen storage in metal–organic frameworks and covalent organic frameworks, Chem. Soc. Rev. 38 (5) (2009) 1460–1476, https://doi.org/10.1039/B802430H.

[20] C. Weidenthaler, M. Felderhoff, Solid-state hydrogen storage for mobile applications: Quo Vadis? Energy Environ. Sci. 4 (7) (2011) 2495–2502, https://doi.org/10.1039/C0EE00771D.

[21] B. Chen, Z. Liu, C. Li, Y. Zhu, L. Fu, Y. Wu, T. van Ree, 9 - Metal oxides for hydrogen storage, in: Y. Wu (Ed.), Metal Oxides in Energy Technologies, Elsevier, 2018, pp. 251–274, https://doi.org/10.1016/B978-0-12-811167-3.00009-2.

[22] A. Salehabadi, E.A. Dawi, D.A. Sabur, W.K. Al-Azzawi, M. Salavati-Niasari, Progress on nano-scaled alloys and mixed metal oxides in solid-state hydrogen storage; an overview, J. Energy Storage 61 (2023), 106722, https://doi.org/10.1016/j.est.2023.106722.

[23] Z. Wang, F. Wang, M. Li, M.Z. Iqbal, Y. Lu, M. Xu, Q. Li, Synthesis, characterization and hydrogen storage characteristics of flower-like SnO_2 porous microspheres, Mater. Lett. 119 (2014) 36–38, https://doi.org/10.1016/j.matlet.2013.12.101.

[24] T. Gholami, M. Salavati-Niasari, S. Varshoy, Electrochemical hydrogen storage capacity and optical properties of $NiAl_2O_4$/NiO nanocomposite synthesized by green method, Int. J. Hydrog. Energy 42 (8) (2017) 5235–5245, https://doi.org/10.1016/j.ijhydene.2016.10.132.

[25] V.A. Yartys, M.V. Lototskyy, E. Akiba, R. Albert, V.E. Antonov, J.R. Ares, M. Baricco, N. Bourgeois, C.E. Buckley, J.M. Bellosta von Colbe, J.C. Crivello,

F. Cuevas, R.V. Denys, M. Dornheim, M. Felderhoff, D.M. Grant, B.C. Hauback, T. D. Humphries, I. Jacob, T.R. Jensen, P.E. de Jongh, J.M. Joubert, M. A. Kuzovnikov, M. Latroche, M. Paskevicius, L. Pasquini, L. Popilevsky, V. M. Skripnyuk, E. Rabkin, M.V. Sofianos, A. Stuart, G. Walker, H. Wang, C. J. Webb, M. Zhu, Magnesium based materials for hydrogen based energy storage: past, present and future, Int. J. Hydrog. Energy 44 (15) (2019) 7809–7859, https://doi.org/10.1016/j.ijhydene.2018.12.212.

[26] H. Liu, P. Sun, R.C. Bowman, Z.Z. Fang, Y. Liu, C. Zhou, Effect of air exposure on hydrogen storage properties of catalyzed magnesium hydride, J. Power Sources 454 (2020), 227936, https://doi.org/10.1016/j.jpowsour.2020.227936.

[27] C.-Y. Seo, J.-H. Kim, P.S. Lee, J.-Y. Lee, Hydrogen storage properties of vanadium-based b.c.c. solid solution metal hydrides, J. Alloys Compd. 348 (1) (2003) 252–257, https://doi.org/10.1016/S0925-8388(02)00831-9.

[28] S. Kumar, A. Jain, T. Ichikawa, Y. Kojima, G.K. Dey, Development of vanadium based hydrogen storage material: a review, Renew. Sust. Energ. Rev. 72 (2017) 791–800, https://doi.org/10.1016/j.rser.2017.01.063.

[29] G.K. Sujan, Z. Pan, H. Li, D. Liang, N. Alam, An overview on TiFe intermetallic for solid-state hydrogen storage: microstructure, hydrogenation and fabrication processes, Crit. Rev. Solid State Mater. Sci. 45 (5) (2020) 410–427, https://doi.org/10.1080/10408436.2019.1652143.

[30] E.M. Dematteis, N. Berti, F. Cuevas, M. Latroche, M. Baricco, Substitutional effects in TiFe for hydrogen storage: a comprehensive review, Mater. Adv. 2 (8) (2021) 2524–2560, https://doi.org/10.1039/D1MA00101A.

[31] Y.-H. Zhang, C. Li, Z.-M. Yuan, Y. Qi, S.-H. Guo, D.-L. Zhao, Research progress of TiFe-based hydrogen storage alloys, J. Iron Steel Res. Int. 29 (4) (2022) 537–551, https://doi.org/10.1007/s42243-022-00756-w.

[32] J. Prigent, J.M. Joubert, M. Gupta, Modification of the hydrogenation properties of $LaNi_5$ upon Ni substitution by Rh, Ir, Pt or Au, J. Alloys Compd. 511 (1) (2012) 95–100, https://doi.org/10.1016/j.jallcom.2011.08.094.

[33] M. Spodaryk, N. Gasilova, A. Züttel, Hydrogen storage and electrochemical properties of $LaNi_{5-x}Cu_x$ hydride-forming alloys, J. Alloys Compd. 775 (2019) 175–180, https://doi.org/10.1016/j.jallcom.2018.10.009.

[34] B. Bogdanović, M. Felderhoff, A. Pommerin, F. Schüth, N. Spielkamp, Advanced hydrogen-storage materials based on Sc-, Ce-, and Pr-doped $NaAlH_4$, Adv. Mater. 18 (9) (2006) 1198–1201, https://doi.org/10.1002/adma.200501367.

[35] J. Chen, N. Kuriyama, Q. Xu, H.T. Takeshita, T. Sakai, Reversible hydrogen storage via titanium-catalyzed $LiAlH_4$ and Li_3AlH_6, J. Phys. Chem. B 105 (45) (2001) 11214–11220, https://doi.org/10.1021/jp012127w.

[36] A. Züttel, P. Wenger, S. Rentsch, P. Sudan, P. Mauron, C. Emmenegger, $LiBH_4$ a new hydrogen storage material, J. Power Sources 118 (1) (2003) 1–7, https://doi.org/10.1016/S0378-7753(03)00054-5.

[37] A. Kantürk Figen, M.B. Pişkin, B. Coşkuner, V. İmamoğlu, Synthesis, structural characterization, and hydrolysis of Ammonia Borane (NH_3BH_3) as a hydrogen storage carrier, Int. J. Hydrog. Energy 38 (36) (2013) 16215–16228, https://doi.org/10.1016/j.ijhydene.2013.10.033.

[38] E. Pawelczyk, N. Łukasik, I. Wysocka, A. Rogala, J. Gębicki, Recent progress on hydrogen storage and production using chemical hydrogen carriers, Energies 15 (14) (2022) 4964.

[39] D. Tang, G.-L. Tan, G.-W. Li, J.-G. Liang, S.M. Ahmad, A. Bahadur, M. Humayun, H. Ullah, A. Khan, M. Bououdina, State-of-the-art hydrogen generation techniques and storage methods: a critical review, J. Energy Storage 64 (2023), 107196, https://doi.org/10.1016/j.est.2023.107196.

[40] B. Sakintuna, F. Lamari-Darkrim, M. Hirscher, Metal hydride materials for solid hydrogen storage: a review, Int. J. Hydrog. Energy 32 (9) (2007) 1121–1140, https://doi.org/10.1016/j.ijhydene.2006.11.022.

[41] N. Stetson, An overview of US DOE's activities for hydrogen fuel cell technologies, in: Proceedings of the Materials Challenges in Alternative & Renewable Energy Conference, 2012, pp. 1–41.

[42] J. Ren, N.M. Musyoka, H.W. Langmi, M. Mathe, S. Liao, Current research trends and perspectives on materials-based hydrogen storage solutions: a critical review, Int. J. Hydrog. Energy 42 (1) (2017) 289–311, https://doi.org/10.1016/j.ijhydene.2016.11.195.

[43] N.A.A. Rusman, M. Dahari, A review on the current progress of metal hydrides material for solid-state hydrogen storage applications, Int. J. Hydrog. Energy 41 (28) (2016) 12108–12126, https://doi.org/10.1016/j.ijhydene.2016.05.244.

[44] T.K. Mandal, D.H. Gregory, Hydrogen storage materials: present scenarios and future directions, annual reports section "A", Inorg. Chem. 105 (0) (2009) 21–54, https://doi.org/10.1039/B818951J.

[45] W. Jiang, H. Wang, M. Zhu, AlH_3 as a hydrogen storage material: recent advances, prospects and challenges, Rare Metals 40 (12) (2021) 3337–3356, https://doi.org/10.1007/s12598-021-01769-2.

[46] M. Dornheim, Thermodynamics of Metal Hydrides: Tailoring Reaction Enthalpies of Hydrogen Storage Materials, Thermodynamics-Interaction Studies-Solids, Liquids and Gases, IntechOpen, 2011, https://doi.org/10.5772/21662.

[47] G.G. Libowitz, Metallic hydrides; fundamental properties and applications, J. Phys. Chem. Solids 55 (12) (1994) 1461–1470, https://doi.org/10.1016/0022-3697(94)90571-1.

[48] A. Züttel, Materials for hydrogen storage, Mater. Today 6 (9) (2003) 24–33, https://doi.org/10.1016/S1369-7021(03)00922-2.

[49] A.R. Miedema, The electronegativity parameter for transition metals: heat of formation and charge transfer in alloys, J. Less-Common Met. 32 (1) (1973) 117–136, https://doi.org/10.1016/0022-5088(73)90078-7.

[50] J. Bellosta von Colbe, J.-R. Ares, J. Barale, M. Baricco, C. Buckley, G. Capurso, N. Gallandat, D.M. Grant, M.N. Guzik, I. Jacob, E.H. Jensen, T. Jensen, J. Jepsen, T. Klassen, M.V. Lototskyy, K. Manickam, A. Montone, J. Puszkiel, S. Sartori, D. A. Sheppard, A. Stuart, G. Walker, C.J. Webb, H. Yang, V. Yartys, A. Züttel, M. Dornheim, Application of hydrides in hydrogen storage and compression: achievements, outlook and perspectives, Int. J. Hydrog. Energy 44 (15) (2019) 7780–7808, https://doi.org/10.1016/j.ijhydene.2019.01.104.

[51] M.V. Lototskyy, I. Tolj, M.W. Davids, Y.V. Klochko, A. Parsons, D. Swanepoel, R. Ehlers, G. Louw, B. van der Westhuizen, F. Smith, B.G. Pollet, C. Sita, V. Linkov, Metal hydride hydrogen storage and supply systems for electric forklift with low-temperature proton exchange membrane fuel cell power module, Int. J. Hydrog. Energy 41 (31) (2016) 13831–13842, https://doi.org/10.1016/j.ijhydene.2016.01.148.

[52] M.V. Lototskyy, I. Tolj, L. Pickering, C. Sita, F. Barbir, V. Yartys, The use of metal hydrides in fuel cell applications, Prog. Nat. Sci.: Mater. Int. 27 (1) (2017) 3–20, https://doi.org/10.1016/j.pnsc.2017.01.008.

[53] H.H. Van Mal, K.H.J. Buschow, A.R. Miedema, Hydrogen absorption in $LaNi_5$ and related compounds: experimental observations and their explanation, J. Less-Common Met. 35 (1) (1974) 65–76, https://doi.org/10.1016/0022-5088(74)90146-5.

[54] J.J. Reilly, R.H. Wiswall, Formation and properties of iron titanium hydride, Inorg. Chem. 13 (1) (1974) 218–222, https://doi.org/10.1021/ic50131a042.

[55] G. Sandrock, A panoramic overview of hydrogen storage alloys from a gas reaction point of view, J. Alloys Compd. 293-295 (1999) 877–888, https://doi.org/10.1016/S0925-8388(99)00384-9.

[56] J. Chen, H.T. Takeshita, H. Tanaka, N. Kuriyama, T. Sakai, I. Uehara, M. Haruta, Hydriding properties of $LaNi_3$ and $CaNi_3$ and their substitutes with $PuNi_3$-type structure, J. Alloys Compd. 302 (1) (2000) 304–313, https://doi.org/10.1016/S0925-8388(00)00694-0.

[57] L. Luo, F. Yang, Y. Li, L. Li, Y. Li, Investigation of the microstructure and hydrogen storage behavior of $V_{48}Fe_{12}Ti_{15+x}Cr_{25-x}$ (x=0, 5, 10, 15) alloys, Int. J. Hydrog. Energy 47 (16) (2022) 9653–9671, https://doi.org/10.1016/j.ijhydene.2022.01.058.

[58] P. Edalati, R. Floriano, A. Mohammadi, Y. Li, G. Zepon, H.-W. Li, K. Edalati, Reversible room temperature hydrogen storage in high-entropy alloy TiZrCrMnFeNi, Scr. Mater. 178 (2020) 387–390, https://doi.org/10.1016/j.scriptamat.2019.12.009.

[59] P. Modi, K.-F. Aguey-Zinsou, Room temperature metal hydrides for stationary and heat storage applications: a review, Front. Energy Res. 9 (2021), https://doi.org/10.3389/fenrg.2021.616115.

[60] H. Liu, J. Zhang, C. Zhou, P. Sun, Y. Liu, Z.Z. Fang, Hydrogen storage properties of Ti-Fe-Zr-Mn-Nb alloys, J. Alloys Compd. 938 (2023), 168466, https://doi.org/10.1016/j.jallcom.2022.168466.

[61] F. Laves, H.J. Wallbaum, Zur Kristallchemie von Titan-Legierungen, Naturwissenschaften 27 (1939) 674–675, https://doi.org/10.1007/bf01494992.

[62] A.M. Van der Kraan, K.H.J. Buschow, The 57Fe Mössbauer isomer shift in intermetallic compounds of iron, Phys. B+C 138 (1) (1986) 55–62, https://doi.org/10.1016/0378-4363(86)90492-4.

[63] P. Thompson, M.A. Pick, F. Reidinger, L.M. Corliss, J.M. Hastings, J.J. Reilly, Neutron diffraction study of β iron titanium deuteride, J. Phys. F: Met. Phys. 8 (4) (1978) L75, https://doi.org/10.1088/0305-4608/8/4/001.

[64] P. Fischer, W. Hälg, L. Schlapbach, F. Stucki, A.F. Andresen, Deuterium storage in FeTi. Measurement of desorption isotherms and structural studies by means of neutron diffraction, Mater. Res. Bull. 13 (9) (1978) 931–946, https://doi.org/10.1016/0025-5408(78)90105-8.

[65] G. Sandrock, State-of-the-Art Review of Hydrogen Storage in Reversible Metal Hydrides for Military Fuel Cell Applications, SUNATECH INC., Fort Belvoir, VA, 1997.

[66] A. Dwight, CsCl-type equiatomic phases in binary alloys of transition elements, Trans. Am. Inst. Min. Metall. Eng. 215 (2) (1959) 283–286.

[67] K. Yvon, P. Fischer, Crystal and magnetic structures of ternary metal hydrides: a comprehensive review, in: L. Schlapbach (Ed.), Hydrogen in Intermetallic Compounds I: Electronic, Thermodynamic, and Crystallographic Properties, Preparation, Springer, Berlin Heidelberg, Berlin, Heidelberg, 1988, pp. 87–138, https://doi.org/10.1007/3540183337_11.

[68] W.-S. Ko, K.B. Park, H.-K. Park, Density functional theory study on the role of ternary alloying elements in TiFe-based hydrogen storage alloys, J. Mater. Sci. Technol. 92 (2021) 148–158, https://doi.org/10.1016/j.jmst.2021.03.042.

[69] J. Reilly, Metal Hydrides as Hydrogen Storage Media and Their Applications, Brookhaven National Lab, Upton, NY (USA), 1976, https://doi.org/10.2172/7268032.

[70] P. Fischer, J. Schefer, K. Yvon, L. Schlapbach, T. Riesterer, Orthorhombic structure of γ-TiFeD≈2, J. Less-Common Met. 129 (1987) 39–45, https://doi.org/10.1016/0022-5088(87)90031-2.

[71] H. Liu, J. Zhang, P. Sun, C. Zhou, Y. Liu, Z.Z. Fang, Effect of oxygen on the hydrogen storage properties of TiFe alloys, J. Energy Storage 55 (2022), 105543, https://doi.org/10.1016/j.est.2022.105543.

[72] P.D. Goodell, G.D. Sandrock, E.L. Huston, Kinetic and dynamic aspects of rechargeable metal hydrides, J. Less-Common Met. 73 (1) (1980) 135–142, https://doi.org/10.1016/0022-5088(80)90352-5.

[73] E.M. Dematteis, D.M. Dreistadt, G. Capurso, J. Jepsen, F. Cuevas, M. Latroche, Fundamental hydrogen storage properties of TiFe-alloy with partial substitution of Fe by Ti and Mn, J. Alloys Compd. 874 (2021), 159925, https://doi.org/10.1016/j.jallcom.2021.159925.

[74] M.H. Mintz, S. Vaknin, S. Biderman, Z. Hadari, Hydrides of ternary $TiFe_xM_{1-x}$(M=Cr, Mn, Co, Ni) intermetallics, J. Appl. Phys. 52 (1) (1981) 463–467, https://doi.org/10.1063/1.329808.

[75] A. Guéguen, M. Latroche, Influence of the addition of vanadium on the hydrogenation properties of the compounds $TiFe_{0.9}V_x$ and $TiFe_{0.8}Mn_{0.1}V_x$ (x=0,

0.05 and 0.1), J. Alloys Compd. 509 (18) (2011) 5562–5566, https://doi.org/10.1016/j.jallcom.2011.02.036.
[76] A. Lys, J.O. Fadonougbo, M. Faisal, J.-Y. Suh, Y.-S. Lee, J.-H. Shim, J. Park, Y. W. Cho, Enhancing the hydrogen storage properties of A_xB_y intermetallic compounds by partial substitution: a short review, Hydrogen 1 (1) (2020) 38–63, https://doi.org/10.3390/hydrogen1010004.
[77] C.E. Lundin, F.E. Lynch, C.B. Magee, A correlation between the interstitial hole sizes in intermetallic compounds and the thermodynamic properties of the hydrides formed from those compounds, J. Less-Common Met. 56 (1) (1977) 19–37, https://doi.org/10.1016/0022-5088(77)90215-6.
[78] E.M. Dematteis, F. Cuevas, M. Latroche, Hydrogen storage properties of Mn and Cu for Fe substitution in $TiFe_{0.9}$ intermetallic compound, J. Alloys Compd. 851 (2021), 156075, https://doi.org/10.1016/j.jallcom.2020.156075.
[79] W. Ali, Z. Hao, Z. Li, G. Chen, Z. Wu, X. Lu, C. Li, Effects of Cu and Y substitution on hydrogen storage performance of $TiFe_{0.86}Mn_{0.1}Y_{0.1-x}Cu_x$, Int. J. Hydrog. Energy 42 (26) (2017) 16620–16631, https://doi.org/10.1016/j.ijhydene.2017.04.247.
[80] W. Ali, M. Li, P. Gao, C. Wu, Q. Li, X. Lu, C. Li, Hydrogenation properties of Ti-Fe-Mn alloy with cu and Y as additives, Int. J. Hydrog. Energy 42 (4) (2017) 2229–2238, https://doi.org/10.1016/j.ijhydene.2016.09.037.
[81] J.O. Fadonougbo, K.B. Park, T.-W. Na, C.-S. Park, H.-K. Park, W.-S. Ko, An integrated computational and experimental method for predicting hydrogen plateau pressures of $TiFe_{1-x}M_x$-based room temperature hydrides, Int. J. Hydrog. Energy 47 (40) (2022) 17673–17682, https://doi.org/10.1016/j.ijhydene.2022.03.240.
[82] V. Kumar, P. Kumar, K. Takahashi, P. Sharma, Hydrogen adsorption studies of TiFe surfaces via 3-d transition metal substitution, Int. J. Hydrog. Energy 47 (36) (2022) 16156–16164, https://doi.org/10.1016/j.ijhydene.2022.03.138.
[83] A. Mohammadi, Y. Ikeda, P. Edalati, M. Mito, B. Grabowski, H.-W. Li, K. Edalati, High-entropy hydrides for fast and reversible hydrogen storage at room temperature: binding-energy engineering via first-principles calculations and experiments, Acta Mater. 236 (2022), 118117, https://doi.org/10.1016/j.actamat.2022.118117.
[84] R. Floriano, G. Zepon, K. Edalati, G.L.B.G. Fontana, A. Mohammadi, Z. Ma, H.-W. Li, R.J. Contieri, Hydrogen storage in TiZrNbFeNi high entropy alloys, designed by thermodynamic calculations, Int. J. Hydrog. Energy 45 (58) (2020) 33759–33770, https://doi.org/10.1016/j.ijhydene.2020.09.047.
[85] H.Y. Zhu, J. Wu, Q.D. Wang, Reactivation behaviour of TiFe hydride, J. Alloys Compd. 215 (1) (1994) 91–95, https://doi.org/10.1016/0925-8388(94)90823-0.
[86] T. Hirata, Decomposition of the $FeTi_{1.13}$ hydride after hydrogen absorption-desorption cycles in oxygen-contaminated hydrogen, J. Less-Common Met. 113 (2) (1985) 189–196, https://doi.org/10.1016/0022-5088(85)90276-0.
[87] X.-N. Yu, Z. Lin, Surface properties on hydrogen storage material TiFeMm, J. Less-Common Met. 130 (1987) 535–540, https://doi.org/10.1016/0022-5088(87)90153-6.
[88] G.D. Sandrock, P.D. Goodell, Cyclic life of metal hydrides with impure hydrogen: overview and engineering considerations, J. Less-Common Met. 104 (1) (1984) 159–173, https://doi.org/10.1016/0022-5088(84)90452-1.
[89] P. Modi, K.-F. Aguey-Zinsou, Titanium-iron-manganese ($TiFe_{0.85}Mn_{0.15}$) alloy for hydrogen storage: reactivation upon oxidation, Int. J. Hydrog. Energy 44 (31) (2019) 16757–16764, https://doi.org/10.1016/j.ijhydene.2019.05.005.
[90] L. Schlapbach, A. Seiler, F. Stucki, H.C. Siegmann, Surface effects and the formation of metal hydrides, J. Less-Common Met. 73 (1) (1980) 145–160, https://doi.org/10.1016/0022-5088(80)90354-9.
[91] T. Schober, D. Westlake, Activation of FeTi for hydrogen storage: a different view, Scr. Metall. 15 (8) (1981), https://doi.org/10.1016/0036-9748(81)90277-5.
[92] L. Schlapbach, T. Riesterer, The activation of FeTi for hydrogen absorption, Appl. Phys. A Mater. Sci. Process. 32 (4) (1983) 169–182, https://doi.org/10.1007/BF00820257.
[93] H. Züchner, U. Bilitewski, G. Kirch, Auger electron spectroscopy and secondary ion mass spectrometry investigations of the activation of TiFe for hydrogen uptake, J. Less-Common Met. 101 (1984) 441–451, https://doi.org/10.1016/0022-5088(84)90120-6.
[94] G. Sandrock, J. Reilly, J. Johnson, Metallurgical Considerations in the Production and Use of FeTi Alloys for Hydrogen Storage, Brookhaven National Lab, Upton, NY (USA), 1976.
[95] T. Matsumoto, M. Amano, The hydriding of FeTi during an activation treatment-by in-situ X-ray diffraction, Scr. Metall. 15 (8) (1981) 879–883, https://doi.org/10.1016/0036-9748(81)90270-2.
[96] C.S. Pande, M.A. Pick, R.L. Sabatini, The "activation" of FeTi for hydrogen absorption; An electron microscopic study, Scr. Metall. 14 (8) (1980) 899–903, https://doi.org/10.1016/0036-9748(80)90317-8.
[97] K.B. Park, J.O. Fadonougbo, J.-S. Bae, G.B. Kang, J.I. Choi, Y.D. Kim, T.-W. Na, H.-K. Park, The evolution of surface oxides during $TiFe_{0.9}M_{0.1}$ (M = Ni, Mn) activation: an in situ XPS investigation, Metals 12 (12) (2022) 2093, https://doi.org/10.3390/met12122093.
[98] J.J. Reilly, J.R. Johnson, F. Reidinger, J.F. Lynch, J. Tanaka, R.H. Wiswall, Lattice expansion as a measure of surface segregation and the solubility of hydrogen in α-$FeTiH_x$, J. Less-Common Met. 73 (1) (1980) 175–182, https://doi.org/10.1016/0022-5088(80)90358-6.
[99] H.C. Siegmann, L. Schlapbach, C.R. Brundle, Self-restoring of the active surface in the hydrogen sponge $LaNi_5$, Phys. Rev. Lett. 40 (14) (1978) 972–975, https://doi.org/10.1103/PhysRevLett.40.972.
[100] L. Schlapbach, A. Seiler, F. Stucki, Surface segregation in FeTi and its catalytic effect on the hydrogenation II: AES and XPS studies, Mater. Res. Bull. 13 (10) (1978) 1031–1037, https://doi.org/10.1016/0025-5408(78)90168-X.
[101] F. Stucki, L. Schlapbach, Magnetic properties of $LaNi_5$, FeTi, Mg2Ni and their hydrides, J. Less-Common Met. 74 (1) (1980) 143–151, https://doi.org/10.1016/0022-5088(80)90084-3.
[102] A. Bläsius, U. Gonster, Mössbauer surface studies on Tife hydrogen storage material, Appl. Phys. 22 (3) (1980) 331–332, https://doi.org/10.1007/BF00899887.
[103] G. Busch, L. Schlapbach, F. Stucki, P. Fischer, A.F. Andresen, Hydrogen storage in FeTi: surface segregation and its catalytic effect on hydrogenation and structural studies by means of neutron diffraction, Int. J. Hydrog. Energy 4 (1) (1979) 29–39, https://doi.org/10.1016/0360-3199(79)90127-7.
[104] L. Schlapbach, A. Seiler, F. Stucki, P. Zürcher, P. Fischer, J. Schefer, How FeTi absorbs hydrogen, Z. Phys. Chem. 117 (117) (1979) 205–220, https://doi.org/10.1524/zpch.1979.117.117.205.
[105] K. Edalati, J. Matsuda, M. Arita, T. Daio, E. Akiba, Z. Horita, Mechanism of activation of TiFe intermetallics for hydrogen storage by severe plastic deformation using high-pressure torsion, Appl. Phys. Lett. 103 (14) (2013), https://doi.org/10.1063/1.4823555.
[106] D. Fruchart, M. Commandré, D. Sauvage, A. Rouault, R. Tellgren, Structural and activation process studies of FeTi-like hydride compounds, J. Less-Common Met. 74 (1) (1980) 55–63, https://doi.org/10.1016/0022-5088(80)90073-9.
[107] T. Schober, On the activation of FeTi for hydrogen storage, J. Less-Common Met. 89 (1) (1983) 63–70, https://doi.org/10.1016/0022-5088(83)90249-7.
[108] Y. Shenzhong, Y. Rong, H. Tiesheng, Z. Shilong, C. Bingzhao, A study of the activation of FeTi and $Fe_{0.9}$ $TiMn_{0.1}$, Int. J. Hydrog. Energy 13 (7) (1988) 433–437, https://doi.org/10.1016/0360-3199(88)90129-2.
[109] K. Hiebl, E. Tuscher, H. Bittner, Untersuchungen an Hydriden im Bereich der η-Phase Ti_4Fe_2O, Monatsh. Chem. 110 (1) (1979) 9–19, https://doi.org/10.1007/BF00903742.
[110] M.H. Mintz, Z. Hadari, M.P. Dariel, Hydrogenation of oxygen-stabilized Ti_2MO_x (M = Fe, Co, Ni; $0 \leqslant_x < 0.5$) compounds, J. Less-Common Met. 74 (2) (1980) 287–294, https://doi.org/10.1016/0022-5088(80)90164-2.
[111] B. Rupp, On the change in physical properties of $Ti_{4-x}Fe_{2+x}O_y$ during hydrogenation I: activation behaviour of ternary oxides $Ti_{4-x}Fe_{2+x}O_y$ and β-Ti, J. Less-Common Met. 104 (1) (1984) 51–63, https://doi.org/10.1016/0022-5088(84)90435-1.
[112] A. Venkert, M. Talianker, M.P. Dariel, A tem study of activated FeTi surface, Mater. Lett. 2 (1) (1983) 45–48, https://doi.org/10.1016/0167-577X(83)90030-7.
[113] J. Huot, F. Cuevas, S. Deledda, K. Edalati, Y. Filinchuk, T. Grosdidier, B. C. Hauback, M. Heere, T.R. Jensen, M. Latroche, S. Sartori, Mechanochemistry of metal hydrides: recent advances, Materials 12 (17) (2019) 2778, https://doi.org/10.3390/ma12172778.
[114] E. Ulate-Kolitsky, B. Tougas, J. Huot, First hydrogenation of TiFe with addition of 20 wt.% Ti, Hydrogen 3 (4) (2022) 379–388, https://doi.org/10.3390/hydrogen3040023.
[115] S.M. Lee, T.P. Perng, Microstructural correlations with the hydrogenation kinetics of $FeTi_{1+\xi}$ alloys, J. Alloys Compd. 177 (1) (1991) 107–118, https://doi.org/10.1016/0925-8388(91)90061-Y.
[116] T. Suda, M. Ohkawa, S. Sawada, S. Watanabe, S. Ohnuki, S. Nagata, Effect of surface modification by ion implantation on hydrogenation property of TiFe alloy, Mater. Trans. 43 (11) (2002) 2703–2705, https://doi.org/10.2320/matertrans.43.2703.
[117] M. Williams, M.V. Lototsky, M.W. Davids, V. Linkov, V.A. Yartys, J.K. Solberg, Chemical surface modification for the improvement of the hydrogenation kinetics and poisoning resistance of TiFe, J. Alloys Compd. 509 (2011) S770–S774, https://doi.org/10.1016/j.jallcom.2010.11.063.
[118] T. Bratanich, S. Solonin, V. Skorokhod, Hydrogen sorption peculiarities of mechanically activated intermetallic TiFe and TiFe-$MmNi_5$($LaNi_5$) mixtures, Int. J. Hydrog. Energy 21 (11) (1996) 1049–1051, https://doi.org/10.1016/S0360-3199(96)00042-0.
[119] H. Emami, K. Edalati, J. Matsuda, E. Akiba, Z. Horita, Hydrogen storage performance of TiFe after processing by ball milling, Acta Mater. 88 (2015) 190–195, https://doi.org/10.1016/j.actamat.2014.12.052.
[120] F. Guo, K. Namba, H. Miyaoka, A. Jain, T. Ichikawa, Hydrogen storage behavior of TiFe alloy activated by different methods, Mater. Lett. X 9 (2021), 100061, https://doi.org/10.1016/j.mlblux.2021.100061.
[121] K. Edalati, J. Matsuda, H. Iwaoka, S. Toh, E. Akiba, Z. Horita, High-pressure torsion of TiFe intermetallics for activation of hydrogen storage at room temperature with heterogeneous nanostructure, Int. J. Hydrog. Energy 38 (11) (2013) 4622–4627, https://doi.org/10.1016/j.ijhydene.2013.01.185.
[122] L.E.R. Vega, D.R. Leiva, R.M. Leal Neto, W.B. Silva, R.A. Silva, T.T. Ishikawa, C. S. Kiminami, W.J. Botta, Mechanical activation of TiFe for hydrogen storage by cold rolling under inert atmosphere, Int. J. Hydrog. Energy 43 (5) (2018) 2913–2918, https://doi.org/10.1016/j.ijhydene.2017.12.054.
[123] M. Polanski, M. Kwiatkowska, I. Kunce, J. Bystrzycki, Combinatorial synthesis of alloy libraries with a progressive composition gradient using laser engineered net shaping (LENS): hydrogen storage alloys, Int. J. Hydrog. Energy 38 (27) (2013) 12159–12171, https://doi.org/10.1016/j.ijhydene.2013.05.024.
[124] Y. Shang, S. Liu, Z. Liang, F. Pyczak, Z. Lei, T. Heidenreich, A. Schökel, J.-J. Kai, G. Gizer, M. Dornheim, T. Klassen, C. Pistidda, Developing sustainable FeTi alloys for hydrogen storage by recycling, Commun. Mater. 3 (1) (2022) 101, https://doi.org/10.1038/s43246-022-00324-5.
[125] J. Barale, E.M. Dematteis, G. Capurso, B. Neuman, S. Deledda, P. Rizzi, F. Cuevas, M. Baricco, $TiFe_{0.85}Mn_{0.05}$ alloy produced at industrial level for a hydrogen storage plant, Int. J. Hydrog. Energy 47 (69) (2022) 29866–29880, https://doi.org/10.1016/j.ijhydene.2022.06.295.

[126] C. Suryanarayana, Mechanical alloying and milling, Prog. Mater. Sci. 46 (1) (2001) 1–184, https://doi.org/10.1016/S0079-6425(99)00010-9.

[127] L. Zaluski, S. Hosatte, P. Tessier, D.H. Ryan, J.O. Ström-Olsen, M.L. Trudeau, R. Schulz, Hydrogen absorption in amorphous and nano-crystalline FeTi, Z. Phys. Chem. 183 (1–2) (1994) 45–49, https://doi.org/10.1524/zpch.1994.183.Part_1_2.045.

[128] S. Morris, S.B. Dodd, P.J. Hall, A.J. Mackinnon, L.E.A. Berlouis, The effect of novel processing on hydrogen uptake in FeTi- and magnesium-based alloys, J. Alloys Compd. 293-295 (1999) 458–462, https://doi.org/10.1016/S0925-8388(99)00338-2.

[129] L. Zaluski, A. Zaluska, P. Tessier, J.O. Ström-Olsen, R. Schulz, Nanocrystalline hydrogen absorbing alloys, Mater. Sci. Forum 225-227 (1996) 853–858, https://doi.org/10.4028/www.scientific.net/MSF.225-227.853.

[130] B.L. Chu, S.M. Lee, T.P. Perng, Preparation and hydrogen absorption property of amorphous $Ti_{50}Fe_{50}$, Int. J. Hydrog. Energy 16 (6) (1991) 413–416, https://doi.org/10.1016/0360-3199(91)90141-5.

[131] M. Abe, T. Kuji, Hydrogen absorption of TiFe alloy synthesized by ball milling and post-annealing, J. Alloys Compd. 446-447 (2007) 200–203, https://doi.org/10.1016/j.jallcom.2006.12.063.

[132] H. Hotta, M. Abe, T. Kuji, H. Uchida, Synthesis of Ti–Fe alloys by mechanical alloying, J. Alloys Compd. 439 (1) (2007) 221–226, https://doi.org/10.1016/j.jallcom.2006.05.137.

[133] V.Y. Zadorozhnyy, S.N. Klyamkin, S.D. Kaloshkin, M.Y. Zadorozhnyy, O. V. Bermesheva, Mechanochemical synthesis and hydrogen sorption properties of nanocrystalline TiFe, Inorg. Mater. 47 (10) (2011) 1081–1086, https://doi.org/10.1134/S0020168511100232.

[134] R.B. Falcão, E.D.C.C. Dammann, C.J. da Rocha, R.M.L. Neto, An investigation on the mechanical alloying of TiFe compound by high-energy ball milling, Mater. Sci. Forum 660-661 (2010) 329–334, https://doi.org/10.4028/www.scientific.net/MSF.660-661.329.

[135] L.E.R. Vega, D.R. Leiva, R.M. Leal Neto, W.B. Silva, R.A. Silva, T.T. Ishikawa, C. S. Kiminami, W.J. Botta, Improved ball milling method for the synthesis of nanocrystalline TiFe compound ready to absorb hydrogen, Int. J. Hydrog. Energy 45 (3) (2020) 2084–2093, https://doi.org/10.1016/j.ijhydene.2019.11.035.

[136] K. Edalati, E. Akiba, Z. Horita, High-pressure torsion for new hydrogen storage materials, Sci. Technol. Adv. Mater. 19 (1) (2018) 185–193, https://doi.org/10.1080/14686996.2018.1435131.

[137] E.I.L. Gómez, K. Edalati, F.J. Antiqueira, D.D. Coimbrão, G. Zepon, D.R. Leiva, T. T. Ishikawa, J.M. Cubero-Sesin, W.J. Botta, Synthesis of nanostructured TiFe hydrogen storage material by mechanical alloying via high-pressure torsion, Adv. Eng. Mater. 22 (10) (2020) 2000011, https://doi.org/10.1002/adem.202000011.

[138] Y. Wu, C. Yin, Z. Zou, H. Wei, X. Li, Combustion synthesis of fine TiFe series alloy powder by magnesothermic reduction of ilmenite, Rare Metals 25 (6, Supplement 1) (2006) 280–283, https://doi.org/10.1016/S1001-0521(07)60089-8.

[139] T. Tsuchiya, N. Yasuda, S. Sasaki, N. Okinaka, T. Akiyama, Combustion synthesis of TiFe-based hydrogen storage alloy from titanium oxide and iron, Int. J. Hydrog. Energy 38 (16) (2013) 6681–6686, https://doi.org/10.1016/j.ijhydene.2013.02.106.

[140] M. Deguchi, N. Yasuda, C. Zhu, N. Okinaka, T. Akiyama, Combustion synthesis of TiFe by utilizing magnesiothermic reduction, J. Alloys Compd. 622 (2015) 102–107, https://doi.org/10.1016/j.jallcom.2014.10.051.

[141] R. Wakabayashi, S. Sasaki, T. Akiyama, Self-ignition combustion synthesis of oxygen-doped TiFe, Int. J. Hydrog. Energy 34 (14) (2009) 5710–5715, https://doi.org/10.1016/j.ijhydene.2009.05.098.

[142] R. Wakabayashi, S. Sasaki, I. Saita, M. Sato, H. Uesugi, T. Akiyama, Self-ignition combustion synthesis of TiFe in hydrogen atmosphere, J. Alloys Compd. 480 (2) (2009) 592–595, https://doi.org/10.1016/j.jallcom.2009.02.008.

[143] I. Saita, M. Sato, H. Uesugi, T. Akiyama, Hydriding combustion synthesis of TiFe, J. Alloys Compd. 446-447 (2007) 195–199, https://doi.org/10.1016/j.jallcom.2007.02.150.

[144] M. Ma, D. Wang, X. Hu, X. Jin, G.Z. Chen, A direct electrochemical route from Ilmenite to hydrogen-storage ferrotitanium alloys, Chem. Eur. J. 12 (19) (2006) 5075–5081, https://doi.org/10.1002/chem.200500697.

[145] S. Tan, T. Örs, M.K. Aydınol, T. Öztürk, İ. Karakaya, Synthesis of FeTi from mixed oxide precursors, J. Alloys Compd. 475 (1) (2009) 368–372, https://doi.org/10.1016/j.jallcom.2008.07.018.

[146] M. Panigrahi, E. Shibata, A. Iizuka, T. Nakamura, Production of Fe-Ti alloy from mixed ilmenite and titanium dioxide by direct electrochemical reduction in molten calcium chloride, Electrochim. Acta 93 (2013) 143–151, https://doi.org/10.1016/j.electacta.2013.01.089.

[147] R. Shi, C. Bai, M. Hu, X. Liu, J. Du, Experimental investigation on the formation mechanism of the TiFe alloy by the molten-salt electrolytic titanium concentrate, J. Min. Metall. Sect. B. 47 (2) (2011) 99–104, https://doi.org/10.4028/www.scientific.net/AMR.936.118910.2298/JMMB101012002S.

[148] R.M. Shi, L.F. Bao, B. Zhang, Effect of temperature on the Ti-Fe alloy prepared by molten salt electrolysis, Adv. Mater. Res. 936 (2014) 1189–1194, https://doi.org/10.4028/www.scientific.net/AMR.936.1189.

[149] R.M. Shi, L.F. Bao, B. Zhang, Preparation of Ti-Fe alloy from titanium concentrate by electro-deoxidization in $CaCl_2$, Adv. Mater. Res. 936 (2014) 1195–1200, https://doi.org/10.4028/www.scientific.net/AMR.936.1195.

[150] L. Xiong, Y. Hua, C. Xu, J. Li, Y. Li, Q. Zhang, Z. Zhou, Y. Zhang, J. Ru, Effect of CaO addition on preparation of ferrotitanium from ilmenite by electrochemical reduction in $CaCl_2$-NaCl molten salt, J. Alloys Compd. 676 (2016) 383–389, https://doi.org/10.1016/j.jallcom.2016.03.195.

[151] B. Wang, C.-Y. Chen, J.-Q. Li, L.-Z. Wang, Y.-P. Lan, S.-Y. Wang, Production of Fe–Ti alloys from mixed slag containing titanium and Fe_2O_3 via direct electrochemical reduction in molten calcium chloride, Metals 10 (12) (2020) 1611, https://doi.org/10.3390/met10121611.

[152] S.P. Padhee, U.K. Chanda, R. Singh, A. Roy, B. Mishra, S. Pati, Electro-deoxidation process for producing FeTi from low-grade Ilmenite: tailoring precursor composition for hydrogen storage, J. Sustain. Metall. 7 (3) (2021) 1178–1189, https://doi.org/10.1007/s40831-021-00412-9.

[153] M.W. Davids, M. Lototskyy, B.G. Pollet, Manufacturing of hydride-forming alloys from mixed titanium-iron oxide, Adv. Mater. Res. 746 (2013) 14–22, https://doi.org/10.4028/www.scientific.net/AMR.746.14.

[154] Y. Kobayashi, H.Y. Teah, N. Hanada, Chemical synthesis of unique intermetallic TiFe nanostructures originating from the morphology of oxide precursors, Nanoscale Adv. 3 (18) (2021) 5284–5291, https://doi.org/10.1039/D1NA00251A.

[155] Y. Kobayashi, S. Yamaoka, S. Yamaguchi, N. Hanada, S. Tada, R. Kikuchi, Low-temperature chemical synthesis of intermetallic TiFe nanoparticles for hydrogen absorption, Int. J. Hydrog. Energy 46 (43) (2021) 22611–22617, https://doi.org/10.1016/j.ijhydene.2021.04.083.

[156] L.I. Kivalo, V.V. Skorokhod, N.F. Grigorenko, Volume changes accompanying the sintering of compacts from mixtures of titanium and iron powders, Soviet Powder Metall. Metal Ceram. 21 (5) (1982) 360–364, https://doi.org/10.1007/BF00802103.

[157] L.I. Kivalo, V.V. Skorokhod, V.Y. Petrishchev, Dilatometric investigation of the sintering of compacts from titanium and iron powder mixtures, Soviet Powder Metall. Metal Ceram. 21 (7) (1982) 534–536, https://doi.org/10.1007/BF00802569.

[158] L.I. Kivalo, V.Y. Petrishchev, V.V. Skorokhod, Effect of manganese on sintering processes in the Ti-Fe system, Soviet Powder Metall. Metal Ceram. 25 (1) (1986) 12–14, https://doi.org/10.1007/BF00843007.

[159] L.I. Kivalo, V.V. Pet'kov, A.V. Polenur, V.V. Skorokhod, Effect of manganese on sintering processes in the Ti-Fe system. III. High-temperature x-ray diffraction investigation of the sintering process, Soviet Powder Metall. Metal Ceram. 27 (4) (1988) 279–283, https://doi.org/10.1007/BF00794446.

[160] M.M. Antonova, Y.G. Privalov, Sintering behavior of compacts from a mixture of titanium and iron powders in hydrogen, Soviet Powder Metall. Metal Ceram. 25 (4) (1986) 291–296, https://doi.org/10.1007/BF00794407.

[161] J. Singh, F. Quli, D.E. Wolfe, J.T. Schriempf, J. Singh, An Overview: Electron Beam-Physical Vapor Deposition Technology-Present and Future Applications, 1999.

[162] H. Suematsu, T. Saikusa, T. Suzuki, W. Jiang, K. Yatsui, Preparation of TiFe thin films by pulsed ion beam evaporation, MRS Online Proc. Libr. 697 (1) (2002) 517, https://doi.org/10.1557/PROC-697-P5.17.

[163] T. Suzuki, T. Saikusa, H. Suematu, W. Jiang, K. Yatsui, Preparation of TiFe thin films by intense pulsed ion-beam evaporation, Surf. Coat. Technol. 169-170 (2003) 491–494, https://doi.org/10.1016/S0257-8972(03)00072-0.

[164] V. Razafindramanana, L. Teulé-Gay, J. Huot, J.-L. Bobet, Elaboration of a Model System Multilayered Si (substrate)/TiFe/Zr/Pd Thin Film by Magnetron Sputtering 4(1), 2022, pp. 1–10, https://doi.org/10.33263/Materials41.005.

[165] E. Ulate-Kolitsky, B. Tougas, B. Neumann, C. Schade, J. Huot, First hydrogenation of mechanically processed TiFe-based alloy synthesized by gas atomization, Int. J. Hydrog. Energy 46 (10) (2021) 7381–7389, https://doi.org/10.1016/j.ijhydene.2020.11.237.

[166] N.J. Grant, Rapid solidification of metallic particulates, JOM 35 (1) (1983) 20–27, https://doi.org/10.1007/BF03338180.

[167] L.A. Jacobson, J. McKittrick, Rapid solidification processing, Mater. Sci. Eng. R. Rep. 11 (8) (1994) 355–408, https://doi.org/10.1016/0927-796X(94)90022-1.

[168] D.H. Lee, H.G. Kwon, K.B. Park, H.-T. Im, R.H. Kwak, S.S. Sohn, H.-K. Park, J. O. Fadonougbo, Phase formation behavior and hydrogen sorption characteristics of $TiFe_{0.8}Mn_{0.2}$ powders prepared by gas atomization, Int. J. Hydrog. Energy (2023), https://doi.org/10.1016/j.ijhydene.2023.03.289 (Article in Press).

[169] K.B. Park, J.O. Fadonougbo, T.-W. Na, T.W. Lee, M. Kim, D.H. Lee, H.G. Kwon, C.-S. Park, Y. Do Kim, H.-K. Park, On the first hydrogenation kinetics and mechanisms of a $TiFe_{0.85}Cr_{0.15}$ alloy produced by gas atomization, Mater. Charact. 192 (2022), 112188, https://doi.org/10.1016/j.matchar.2022.112188.

[170] K.B. Park, T.-W. Na, Y.D. Kim, J.-Y. Park, J.-W. Kang, H.-S. Kang, K. Park, H.-K., Park, characterization of microstructure and surface oxide of $Ti_{1.2}Fe$ hydrogen storage alloy, Int. J. Hydrog. Energy 46 (24) (2021) 13082–13087, https://doi.org/10.1016/j.ijhydene.2021.01.105.

[171] D.M. Dreistadt, T.-T. Le, G. Capurso, J.M. Bellosta von Colbe, A. Santhosh, C. Pistidda, N. Scharnagl, H. Ovri, C. Milanese, P. Jerabek, T. Klassen, J. Jepsen, An effective activation method for industrially produced TiFeMn powder for hydrogen storage, J. Alloys Compd. 919 (2022), 165847, https://doi.org/10.1016/j.jallcom.2022.165847.

[172] K. Edalati, M. Matsuo, H. Emami, S. Itano, A. Alhamidi, A. Staykov, D.J. Smith, S.-I. Orimo, E. Akiba, Z. Horita, Impact of severe plastic deformation on microstructure and hydrogen storage of titanium-iron-manganese intermetallics, Scr. Mater. 124 (2016) 108–111, https://doi.org/10.1016/j.scriptamat.2016.07.007.

[173] A.K. Patel, B. Tougas, P. Sharma, J. Huot, Effect of cooling rate on the microstructure and hydrogen storage properties of TiFe with 4 wt% Zr as an additive, J. Mater. Res. Technol. 8 (6) (2019) 5623–5630, https://doi.org/10.1016/j.jmrt.2019.09.030.

[174] N. Nishimiya, T. Wada, A. Matsumoto, K. Tsutsumi, Hydriding characteristics of zirconium-substituted FeTi, J. Alloys Compd. 313 (1) (2000) 53–58, https://doi.org/10.1016/S0925-8388(00)01181-6.

[175] M. Faisal, J.-H. Kim, Y.W. Cho, J.-I. Jang, J.-Y. Suh, J.-H. Shim, Y.-S. Lee, Design of V-substituted TiFe-based alloy for target pressure range and easy activation, Materials 14 (17) (2021) 4829, https://doi.org/10.3390/ma14174829.

[176] K.B. Park, J.O. Fadonougbo, C.-S. Park, J.-H. Lee, T.-W. Na, H.-S. Kang, W.-S. Ko, H.-K. Park, Effect of Fe substitution on first hydrogenation kinetics of TiFe-based hydrogen storage alloys after air exposure, Int. J. Hydrog. Energy 46 (60) (2021) 30780–30789, https://doi.org/10.1016/j.ijhydene.2021.06.188.

[177] J.Y. Jung, S.-I. Lee, M. Faisal, H. Kim, Y.-S. Lee, J.-Y. Suh, J.-H. Shim, J.-Y. Huh, Y. W. Cho, Effect of Cr addition on room temperature hydrogenation of TiFe alloys, Int. J. Hydrog. Energy 46 (37) (2021) 19478–19485, https://doi.org/10.1016/j.ijhydene.2021.03.096.

[178] S.M. Lee, T.P. Perng, Correlation of substitutional solid solution with hydrogenation properties of $TiFe_{1-x}M_x$ (M=Ni, Co, Al) alloys, J. Alloys Compd. 291 (1) (1999) 254–261, https://doi.org/10.1016/S0925-8388(99)00262-5.

[179] E.A. Berdonosova, V.Y. Zadorozhnyy, M.Y. Zadorozhnyy, K.V. Geodakian, M. V. Zheleznyi, A.A. Tsarkov, S.D. Kaloshkin, S.N. Klyamkin, Hydrogen storage properties of TiFe-based ternary mechanical alloys with cobalt and niobium. A thermochemical approach, Int. J. Hydrog. Energy 44 (55) (2019) 29159–29165, https://doi.org/10.1016/j.ijhydene.2019.03.057.

[180] H. Shang, Y. Li, Y. Zhang, D. Zhao, Y. Qi, X. Xu, Investigations on hydrogen storage performances and mechanisms of as-cast $TiFe_{0.8-m}Ni_{0.2}Co_m$ (m=0, 0.03, 0.05 and 0.1) alloys, Int. J. Hydrog. Energy 46 (34) (2021) 17840–17852, https://doi.org/10.1016/j.ijhydene.2021.02.179.

[181] P. Jain, C. Gosselin, J. Huot, Effect of Zr, Ni and Zr_7Ni_{10} alloy on hydrogen storage characteristics of TiFe alloy, Int. J. Hydrog. Energy 40 (47) (2015) 16921–16927, https://doi.org/10.1016/j.ijhydene.2015.06.007.

[182] K.D. Ćirić, A. Kocjan, A. Gradišek, V.J. Koteski, A.M. Kalijadis, V.N. Ivanovski, Z. V. Laušević, D.L. Stojić, A study on crystal structure, bonding and hydriding properties of Ti-Fe-Ni intermetallics-behind substitution of iron by nickel, Int. J. Hydrog. Energy 37 (10) (2012) 8408–8417, https://doi.org/10.1016/j.ijhydene.2012.02.047.

[183] A. Szajek, M. Jurczyk, E. Jankowska, The electronic and electrochemical properties of the TiFe-based alloys, J. Alloys Compd. 348 (1) (2003) 285–292, https://doi.org/10.1016/S0925-8388(02)00802-2.

[184] H. Nagai, M. Nakatsu, K. Shoji, H. Tamura, Effect of simultaneous addition of oxygen with copper or niobium on the hydriding characteristics of FeTi for hydrogen storage, J. Less-Common Met. 119 (1) (1986) 131–142, https://doi.org/10.1016/0022-5088(86)90203-1.

[185] T. Matsumoto, M. Amano, Y. Sasaki, Hydrogenation of FeTi-based alloys containing β-Ti, J. Less-Common Met. 88 (2) (1982) 443–449, https://doi.org/10.1016/0022-5088(82)90255-7.

[186] P. Kuziora, I. Kunce, S. McCain, N.J.E. Adkins, M. Polański, The influence of refractory metals on the hydrogen storage characteristics of FeTi-based alloys prepared by suspended droplet alloying, Int. J. Hydrog. Energy 45 (41) (2020) 21635–21645, https://doi.org/10.1016/j.ijhydene.2020.05.216.

[187] V. Razafindramanana, S. Gorsse, J. Huot, J.L. Bobet, Effect of hafnium addition on the hydrogenation process of TiFe alloy, Energies 12 (18) (2019) 3477.

[188] P. Lv, Z. Liu, Effect of high zirconium content on hydrogenation properties and anti-poisoning ability of air-exposed TiFe alloy, J. Mater. Res. Technol. 8 (6) (2019) 5972–5983, https://doi.org/10.1016/j.jmrt.2019.09.072.

[189] W. Zheng, W. Song, T. Wu, J. Wang, Y. He, X.-G. Lu, Experimental investigation and thermodynamic modeling of the ternary Ti-Fe-Mn system for hydrogen storage applications, J. Alloys Compd. 891 (2022), 161957, https://doi.org/10.1016/j.jallcom.2021.161957.

[190] S.M. Lee, T.P. Perng, Effect of the second phase on the initiation of hydrogenation of $TiFe_{1-x}M_x$ (M = Cr,Mn) alloys, Int. J. Hydrog. Energy 19 (3) (1994) 259–263, https://doi.org/10.1016/0360-3199(94)90095-7.

[191] T. Ha, J.-H. Kim, C. Sun, Y.-S. Lee, D.-I. Kim, J.-Y. Suh, J.-I. Jang, J. Lee, Y. Kim, J.-H. Shim, Crucial role of Ce particles during initial hydrogen absorption of AB-type hydrogen storage alloys, Nano Energy 112 (2023), 108483, https://doi.org/10.1016/j.nanoen.2023.108483.

[192] A.K. Patel, A. Duguay, B. Tougas, C. Schade, P. Sharma, J. Huot, Microstructure and first hydrogenation properties of TiFe alloy with Zr and Mn as additives, Int. J. Hydrog. Energy 45 (1) (2020) 787–797, https://doi.org/10.1016/j.ijhydene.2019.10.239.

[193] R. Shen, C. Pu, X. Xu, Y. Xu, Z. Li, Z. Wu, Effect of Mischmetal introduction on hydrogen storage properties in impure hydrogen gas of Ti-Fe-Mn-Co Alloys, Metals 10 (12) (2020) 1574, https://doi.org/10.3390/met10121574.

[194] J. Manna, J. Huot, Effect of KCl addition on first hydrogenation kinetics of TiFe, Compounds 2 (4) (2022) 240–251, https://doi.org/10.3390/compounds2040020.

[195] T.I. Bratanich, S.M. Solonin, V.V. Skorokhod, Mechanical activation of hydrogen sorption with intermetallic compounds $LaNi_5$ and TiFe in powder systems, Int. J. Hydrog. Energy 20 (5) (1995) 353–355, https://doi.org/10.1016/0360-3199(94)00062-5.

[196] L. Zaluski, P. Tessier, D.H. Ryan, C.B. Doner, A. Zaluska, J.O. Ström-Olsen, M. L. Trudeau, R. Schulz, Amorphous and nanocrystalline Fe–Ti prepared by ball milling, J. Mater. Res. 8 (12) (1993) 3059–3068, https://doi.org/10.1557/JMR.1993.3059.

[197] T. Haraki, K. Oishi, H. Uchida, Y. Miyamoto, M. Abe, T. Kokaji, S. Uchida, Properties of hydrogen absorption by nano-structured FeTi alloys, Int. J. Mater. Res. 99 (5) (2008) 507–512, https://doi.org/10.3139/146.101669.

[198] C.H. Chiang, Z.H. Chin, T.P. Perng, Hydrogenation of TiFe by high-energy ball milling, J. Alloys Compd. 307 (1) (2000) 259–265, https://doi.org/10.1016/S0925-8388(00)00827-6.

[199] A.K. Patel, D. Siemiaszko, J. Dworecka-Wójcik, M. Polański, Just shake or stir. About the simplest solution for the activation and hydrogenation of an FeTi hydrogen storage alloy, Int. J. Hydrog. Energy 47 (8) (2022) 5361–5371, https://doi.org/10.1016/j.ijhydene.2021.11.136.

[200] K. Edalati, A. Bachmaier, V.A. Beloshenko, Y. Beygelzimer, V.D. Blank, W. J. Botta, K. Bryła, J. Čížek, S. Divinski, N.A. Enikeev, Y. Estrin, G. Faraji, R. B. Figueiredo, M. Fuji, T. Furuta, T. Grosdidier, J. Gubicza, A. Hohenwarter, Z. Horita, J. Huot, Y. Ikoma, M. Janeček, M. Kawasaki, P. Král, S. Kuramoto, T. G. Langdon, D.R. Leiva, V.I. Levitas, A. Mazilkin, M. Mito, H. Miyamoto, T. Nishizaki, R. Pippan, V.V. Popov, E.N. Popova, G. Purcek, O. Renk, Á. Révész, X. Sauvage, V. Sklenicka, W. Skrotzki, B.B. Straumal, S. Suwas, L.S. Toth, N. Tsuji, R.Z. Valiev, G. Wilde, M.J. Zehetbauer, X. Zhu, Nanomaterials by severe plastic deformation: review of historical developments and recent advances, Math. Res. Lett. 10 (4) (2022) 163–256, https://doi.org/10.1080/21663831.2022.2029779.

[201] Á. Révész, M. Gajdics, High-pressure torsion of non-equilibrium hydrogen storage materials: a review, Energies 14 (4) (2021) 819, https://doi.org/10.3390/en14040819.

[202] K. Edalati, J. Matsuda, A. Yanagida, E. Akiba, Z. Horita, Activation of TiFe for hydrogen storage by plastic deformation using groove rolling and high-pressure torsion: similarities and differences, Int. J. Hydrog. Energy 39 (28) (2014) 15589–15594, https://doi.org/10.1016/j.ijhydene.2014.07.124.

[203] J. Huot, M. Tousignant, Effect of cold rolling on metal hydrides, Mater. Trans. 60 (8) (2019) 1571–1576, https://doi.org/10.2320/matertrans.MF201939.

[204] P. Lv, J. Huot, Hydrogenation improvement of TiFe by adding $ZrMn_2$, Energy 138 (2017) 375–382, https://doi.org/10.1016/j.energy.2017.07.072.

[205] P. Lv, Z. Liu, V. Dixit, Improved hydrogen storage properties of TiFe alloy by doping (Zr+2V) additive and using mechanical deformation, Int. J. Hydrog. Energy 44 (51) (2019) 27843–27852, https://doi.org/10.1016/j.ijhydene.2019.08.249.

[206] P. Lv, Z. Liu, A.K. Patel, X. Zhou, J. Huot, Influence of ball milling, cold rolling and doping (Zr+2Cr) on microstructure, first hydrogenation properties and anti-poisoning ability of TiFe alloy, Met. Mater. Int. 27 (5) (2021) 1346–1357, https://doi.org/10.1007/s12540-019-00501-1.

[207] J. Manna, B. Tougas, J. Huot, Mechanical activation of air exposed TiFe+4 wt% Zr alloy for hydrogenation by cold rolling and ball milling, Int. J. Hydrog. Energy 43 (45) (2018) 20795–20800, https://doi.org/10.1016/j.ijhydene.2018.09.096.

[208] J. Manna, B. Tougas, J. Huot, First hydrogenation kinetics of Zr and Mn doped TiFe alloy after air exposure and reactivation by mechanical treatment, Int. J. Hydrog. Energy 45 (20) (2020) 11625–11631, https://doi.org/10.1016/j.ijhydene.2020.02.043.

[209] V.B. Oliveira, C.A.G. Beatrice, R.M. Leal Neto, W.B. Silva, L.A. Pessan, W.J. Botta, D.R. Leiva, Hydrogen absorption/desorption behavior of a cold-rolled TiFe intermetallic compound, Mater. Res. 24 (2021), e20210204, https://doi.org/10.1590/1980-5373-MR-2021-0204.

[210] E.M.B. Heller, A.M. Vredenberg, D.O. Boerma, Hydrogen uptake kinetics of Pd coated FeTi films, Appl. Surf. Sci. 253 (2) (2006) 771–777, https://doi.org/10.1016/j.apsusc.2006.01.004.

[211] M.W. Davids, M. Lototskyy, A. Nechaev, Q. Naidoo, M. Williams, Y. Klochko, Surface modification of TiFe hydrogen storage alloy by metal-organic chemical vapour deposition of palladium, Int. J. Hydrog. Energy 36 (16) (2011) 9743–9750, https://doi.org/10.1016/j.ijhydene.2011.05.036.

[212] V.Y. Zadorozhnyy, S.N. Klyamkin, M.Y. Zadorozhnyy, O.V. Bermesheva, S. D. Kaloshkin, Mechanical alloying of nanocrystalline intermetallic compound TiFe doped by aluminum and chromium, J. Alloys Compd. 586 (2014) S56–S60, https://doi.org/10.1016/j.jallcom.2013.01.138.

[213] S.K. Kulshreshtha, R. Sasikala, P. Suryanarayana, A.J. Singh, R.M. Iyer, Studies on hydrogen storage material FeTi: effect of Sn substitution, Mater. Res. Bull. 23 (3) (1988) 333–340, https://doi.org/10.1016/0025-5408(88)90006-2.

[214] H. Shang, Y. Zhang, Y. Li, J. Gao, W. Zhang, X. Wei, Z. Yuan, L. Ju, Effect of Pr content on activation capability and hydrogen storage performances of TiFe alloy, J. Alloys Compd. 890 (2022), 161785, https://doi.org/10.1016/j.jallcom.2021.161785.

[215] J.R. Johnson, J.J. Reilly, Metal Hydride Development Program at Brookhaven National Library, 1977, p. 27568.

[216] J.J. Reilly, J.R. Johnson, J.F. Lynch, F. Reidinger, Irreversible effects in the FeTi-H system, J. Less-Common Met. 89 (2) (1983) 505–512, https://doi.org/10.1016/0022-5088(83)90362-4.

[217] H.J. Ahn, S.M. Lee, L. Jai-Young, Intrinsic degradation of FeTi by thermally induced hydrogen absorption-desorption cycling, J. Less-Common Met. 142 (1988) 253–261, https://doi.org/10.1016/0022-5088(88)90183-X.

[218] J.R. Johnson, J.J. Reilly, The use of manganese substituted ferrotitanium alloys for energy storage, Altern. Energy Sources 8 (1978) 3739–3769, https://doi.org/10.2172/1004984.

[219] M. Ron, Y. Josephy, Cyclic hydrogen sorption stability of TiFe0.8Ni0.2Hx metal hydride*, Z. Phys. Chem. 164 (2) (1989) 1343–1348, https://doi.org/10.1524/zpch.1989.164.Part_2.1343.

[220] J.J. Reilly, J.R. Johnson, Metal hydride materials program at BNL: current status and future plans, in: Conference: Meeting for the Contractors in the ERDA Hydrogen Energy Program, Airlie House, VA, USA, 8 Nov 1976, United States, 1976, p. 8 (p. Medium: ED; Size).

[221] G.D. Sandrock, P.D. Goodell, Surface poisoning of $LaNi_5$, FeTi and (Fe,Mn)Ti by O_2, Co and H_2O, J. Less-Common Met. 73 (1) (1980) 161–168, https://doi.org/10.1016/0022-5088(80)90355-0.

[222] F.J. Salzano, C. Braun, A. Beufrere, S. Srinivasan, G. Strickland, J.J. Reilly, C. Waide, Hydrogen Storage via Metal Hydrides for Utility and Automotive Energy Storage Applications, 1976, p. 26666.

[223] J.J. Reilly, Applications of metal hydrides., U. S. Department of Energy, Washington, D. C., under Contract #EY76-C-02-0016, in: A.F. Andresen, A. J. Maeland (Eds.), Hydrides for Energy Storage, Pergamon, 1978, pp. 527–550, https://doi.org/10.1016/B978-0-08-022715-3.50047-3.
[224] A.H. Beaufrere, F.J. Salzano, R.J. Isler, W.S. Yu, Hydrogen storage via iron-titanium for a 26 MW(e) peaking electric plant, Int. J. Hydrog. Energy 1 (3) (1976) 307–319, https://doi.org/10.1016/0360-3199(76)90025-2.
[225] J.M. Burger, P.A. Lewis, R.J. Isler, F.J. Salzano, J.M. King Jr., Energy storage for utilities via hydrogen systems, in: 9th Intersociety Energy Conversion Engineering Conference, 1974, pp. 26–30.
[226] G. Strickland, J.J. Reilly, R.H. Wiswall, An engineering-scale energy storage reservoir of Iron titanium hydride, in: T.N. Veziroğlu (Ed.), Hydrogen Energy: Part A, Springer US, Boston, MA, 1975, pp. 611–620, https://doi.org/10.1007/978-1-4684-2607-6_43.
[227] G. Sandrock, Applications of hydrides, in: Y. Yürüm (Ed.), Hydrogen Energy System: Production and Utilization of Hydrogen and Future Aspects, Springer, Netherlands, Dordrecht, 1995, pp. 253–280, https://doi.org/10.1007/978-94-011-0111-0_17.
[228] G. Strckland, W.S. Yu, Some Rate and Modeling Studies on the Use of Iron–titanium Hydride as an Energy Storage Medium for Electric Utility Companies, United States, 1977, p. 62, https://doi.org/10.2172/7287680 (p. Medium: ED; Size).
[229] A. Beaufrere, R.S. Yeo, S. Srinivasan, J. McElroy, G. Hart, Hydrogen–halogen energy storage system for electric utility applications, in: Conference: 12. Intersociety Energy Conversion Engineering Conference, Washington, District of Columbia, United States of America (USA), 28 Aug 1977, United States, 1977, p. 5 (p. Medium: ED; Size).
[230] S. Srinivasan, R.S. Yeo, A. Beaufrere, Hydrogen-Halogen Energy Storage System: Preliminary Feasibility and Economic Assessment, United States, 1976, p. 7, https://doi.org/10.2172/7119219 (p. Medium: ED; Size).
[231] J.R. Johnson, J.J. Reilly, Metal Hydride Reasearch and Development Program at Brookhaven National Laboratory, Conference: Chemical Hydrogen Energy Systems Contracts Review, Washington, DC, USA, 28 Nov 1978, United States, 1978, p. 11 (p. Medium: ED; Size).
[232] R.L. Woolley, H.M. Simons, Hydrogen storage in vehicles: an operational comparison of alternative prototypes, in: Conference: Meeting of the Society of Automotive Engineers on combined fuels and powerplant, St. Louis, MO, USA, 8 Jun 1976; Related Information: SAE Paper 760570, Society of Automotive Engineers,Warrendale, PA, United States, 1976, p. 10, https://doi.org/10.4271/760570 (p. Medium: X; Size).
[233] H. Buchner, Results of hydride research and consequences for the development of hydride vehicles, in: NATO Proc. of the 4 th Intern. Symp. on Automotive Propulsion Systems, 1978.
[234] V. Anderson, Hydrogen energy in United States post office delivery systems, Hydrogen Energy Syst. (1979) 1879–1901.
[235] G. Strickland, Hydrogen Storage Devices for Automobiles, United States, 1978, p. 10, https://doi.org/10.2172/6379035 (p. Medium: ED; Size).
[236] H. Buchner, R. Povel, The daimler-benz hydride vehicle project, Int. J. Hydrog. Energy 7 (3) (1982) 259–266, https://doi.org/10.1016/0360-3199(82)90089-1.
[237] H. Buchner, Perspectives for metal hydride technology, Prog. Energy Combust. Sci. 6 (4) (1980) 331–346, https://doi.org/10.1016/0360-1285(80)90009-X.
[238] H. Buchner, The hydrogen/hydride energy concept, Int. J. Hydrog. Energy 3 (4) (1978) 385–406, https://doi.org/10.1016/0360-3199(78)90001-0.
[239] J. Toepler, O. Bernauer, H. Buchner, The use of hydrides in motor vehicles, J. Less-Common Met. 74 (2) (1980) 385–399, https://doi.org/10.1016/0022-5088(80)90177-0.
[240] R. Beneito, J. Vilaplana, S. Gisbert, Electric toy vehicle powered by a PEMFC stack, Int. J. Hydrog. Energy 32 (10) (2007) 1554–1558, https://doi.org/10.1016/j.ijhydene.2006.10.049.
[241] DOE, Technical targets for onboard hydrogen storage for light-duty vehicles. https://energy.gov/eere/fuelcells/doe-technicaltargets-onboard-hydrogen-storage-light-duty-vehicles (Accessed at 06/22/2022).
[242] H. Uchida, T. Haraki, K. Oishi, Y. Miyamoto, M.A.T. Kokaji, S. Uchida, A Wind & Solar Hybrid Energy Storage System Using Nano-Structured Hydrogen Storage Alloy Proceddins International Hydrogen Energy Congress and Exhibition IHEC, 2005.
[243] N. Endo, S. Suzuki, K. Goshome, T. Maeda, Operation of a bench-scale TiFe-based alloy tank under mild conditions for low-cost stationary hydrogen storage, Int. J. Hydrog. Energy 42 (8) (2017) 5246–5251, https://doi.org/10.1016/j.ijhydene.2016.11.088.
[244] N. Endo, E. Shimoda, K. Goshome, T. Yamane, T. Nozu, T. Maeda, Construction and operation of hydrogen energy utilization system for a zero emission building, Int. J. Hydrog. Energy 44 (29) (2019) 14596–14604, https://doi.org/10.1016/j.ijhydene.2019.04.107.
[245] N. Endo, E. Shimoda, K. Goshome, T. Yamane, T. Nozu, T. Maeda, Operation of a stationary hydrogen energy system using TiFe-based alloy tanks under various weather conditions, Int. J. Hydrog. Energy 45 (1) (2020) 207–215, https://doi.org/10.1016/j.ijhydene.2019.10.240.
[246] R. Halıcıoğlu, Ö.F. Selamet, M. Bayrak, Effects of reactor design on TiFe-hydride's hydrogen storage, Int. J. Energy Res. 37 (7) (2013) 698–705, https://doi.org/10.1002/er.2982.
[247] W. Duan, J. Du, Z. Wang, Y. Niu, T. Huang, Z. Li, C. Pu, Z. Wu, Strain variation on the reaction tank of high hydrogen content during hydrogen absorption-desorption cycles, Int. J. Hydrog. Energy 38 (5) (2013) 2347–2351, https://doi.org/10.1016/j.ijhydene.2012.12.011.
[248] M. Matsushita, I. Tajima, M. Abe, H. Tokuyama, Experimental study of porosity and effective thermal conductivity in packed bed of nano-structured FeTi for usage in hydrogen storage tanks, Int. J. Hydrog. Energy 44 (41) (2019) 23239–23248, https://doi.org/10.1016/j.ijhydene.2019.07.037.
[249] A.K. Patel, A. Duguay, B. Tougas, B. Neumann, C. Schade, P. Sharma, J. Huot, Study of the microstructural and first hydrogenation properties of TiFe alloy with Zr, Mn and V as additives, Processes 9 (7) (2021) 1217, https://doi.org/10.3390/pr9071217.
[250] J.M. Bellosta von Colbe, J. Puszkiel, G. Capurso, A. Franz, H.U. Benz, H. Zoz, T. Klassen, M. Dornheim, Scale-up of milling in a 100L device for processing of TiFeMn alloy for hydrogen storage applications: procedure and characterization, Int. J. Hydrog. Energy 44 (55) (2019) 29282–29290, https://doi.org/10.1016/j.ijhydene.2019.01.174.
[251] HyCARE focuses on large-scale, solid-state hydrogen storage, Fuel Cells Bull. 2019 (2) (2019) 11, https://doi.org/10.1016/S1464-2859(19)30068-9.
[252] D.A. Sheppard, M. Paskevicius, T.D. Humphries, M. Felderhoff, G. Capurso, J. Bellosta von Colbe, M. Dornheim, T. Klassen, P.A. Ward, J.A. Teprovich, C. Corgnale, R. Zidan, D.M. Grant, C.E. Buckley, Metal hydrides for concentrating solar thermal power energy storage, Appl. Phys. A Mater. Sci. Process. 122 (4) (2016) 395, https://doi.org/10.1007/s00339-016-9825-0.
[253] C. Corgnale, B. Hardy, T. Motyka, R. Zidan, J. Teprovich, B. Peters, Screening analysis of metal hydride based thermal energy storage systems for concentrating solar power plants, Renew. Sust. Energ. Rev. 38 (2014) 821–833, https://doi.org/10.1016/j.rser.2014.07.049.
[254] M. Felderhoff, R. Urbanczyk, S. Peil, Thermochemical heat storage for high temperature applications – a review, Green 3 (2) (2013) 113–123, https://doi.org/10.1515/green-2013-0011.
[255] P. Feng, Y. Liu, I. Ayub, Z. Wu, F. Yang, Z. Zhang, Techno-economic analysis of screening metal hydride pairs for a 910 MWhth thermal energy storage system, Appl. Energy 242 (2019) 148–156, https://doi.org/10.1016/j.apenergy.2019.03.046.
[256] C. Corgnale, Techno-economic assessment of destabilized Li hydride systems for high temperature thermal energy storage, Inorganics 8 (5) (2020) 30, https://doi.org/10.3390/inorganics8050030.
[257] E. Schwab, E. Wicke, Nitrogen absorption by the intermetallic compound TiFe and catalytic activity in ammonia synthesis, Z. Phys. Chem. 122 (2) (1980) 217–224, https://doi.org/10.1524/zpch.1980.122.2.217.
[258] E. Schwab, E. Wicke, Nitridation mechanisms of Ti alloys with Fe and Ru in regard to the formation of segregation catalysts, Z. Phys. Chem. 142 (1) (1984) 13–27, https://doi.org/10.1524/zpch.1984.142.1.013.
[259] D.I. Kochubei, V.V. Kriventsov, Y.V. Maksimov, M.V. Tsodikov, F.A. Yandieva, V. P. Mordvin, J.A. Navio, I.I. Moiseev, Intermetallic hydrides [$TiFe_{0.95}Zr_{0.03}Mo_{0.02}$] H_x($0 \leq x \leq 2$): the nature of the phase responsible for the selective reduction of CO_2, Kinet. Catal. 44 (2) (2003) 165–174, https://doi.org/10.1023/A:1023392126234.
[260] M.V. Tsodikov, V.Y. Kugel, F.A. Yandieva, V.P. Mordovin, A.E. Gekhman, I. I. Moiseev, Stoichiometric and catalytic CO_2 reductions involving TiFe-containing intermetallic hydrides, Pure Appl. Chem. 76 (9) (2004) 1769–1779, https://doi.org/10.1351/pac200476091769.
[261] T. Kondo, K. Shindo, Y. Sakurai, Dependence of hydrogen storage characteristics of Mg–$TiFe_{0.92}Mn_{0.08}$ composite on amount of $TiFe_{0.92}Mn_{0.08}$, J. Alloys Compd. 404-406 (2005) 511–514, https://doi.org/10.1016/j.jallcom.2004.10.090.
[262] C. Zhou, Z.Z. Fang, C. Ren, J. Li, J. Lu, Effect of Ti intermetallic catalysts on hydrogen storage properties of magnesium hydride, J. Phys. Chem. C 117 (25) (2013) 12973–12980, https://doi.org/10.1021/jp402770p.
[263] R.A. Silva, R.M. Leal Neto, D.R. Leiva, T.T. Ishikawa, C.S. Kiminami, A.M. Jorge, W.J. Botta, Room temperature hydrogen absorption by Mg and MgTiFe nanocomposites processed by high-energy ball milling, Int. J. Hydrog. Energy 43 (27) (2018) 12251–12259, https://doi.org/10.1016/j.ijhydene.2018.04.174.